SIAM J. NUMER. ANAL.
Vol. 60, No. 5, pp. 2592–2625

PML AND HIGH-ACCURACY BOUNDARY INTEGRAL EQUATION SOLVER FOR WAVE SCATTERING BY A LOCALLY DEFECTED PERIODIC SURFACE*

XIUCHEN YU†, GUANGHUI HU‡, WANGTAO LU§, AND ANDREAS RATHSFELD¶

Abstract. This paper studies the perfectly matched layer (PML) method for wave scattering in a half space of a homogeneous medium bounded by a two-dimensional, perfectly conducting, and locally defected periodic surface, and develops a high-accuracy boundary integral equation (BIE) solver. Along the vertical direction, we place a PML to truncate the unbounded domain onto a strip and prove that the PML solution converges to the true solution in the physical subregion of the strip with an error bounded by the reciprocal PML thickness. Laterally, we divide the unbounded strip into three regions: one region containing the defect and two semi-waveguide regions, separated by two vertical line segments. In both semi-waveguides, we prove the well-posedness of an associated scattering problem so as to well define a Neumann-to-Dirichlet (NtD) operator on the associated vertical segment. The two NtD operators, serving as exact lateral boundary conditions, reformulate the unbounded strip problem as a boundary value problem over the defected region. Due to the periodicity of the semi-waveguides, the two NtD operators are related to two different Neumann-marching operators, and either Neumann-marching operator is governed by a nonlinear Riccati equation. It is proved that the Neumann-marching operators are contracting, so that the PML solution decays exponentially fast along both lateral directions. The consequences culminate in two opposite aspects. Negatively, the PML solution cannot converge exponentially to the true solution in the whole physical region of the strip. Positively, from a numerical perspective, the Riccati equations can now be efficiently solved by a recursive doubling procedure and a high-accuracy PML-based BIE method so that the boundary value problem on the defected region can be solved efficiently and accurately. Numerical experiments demonstrate that the PML solution converges exponentially fast to the true solution in any compact subdomain of the strip.

Key words. periodic structure, PML, boundary integral equation, local defect, Riccati equation

MSC codes. 35B27, 78A40, 78M15

DOI. 10.1137/21M1439705

1. Introduction.

Due to its nearly reflectionless absorption of outgoing waves, the perfectly matched layer, or PML, since its invention by Bérenger in 1994 [4], has become a primary truncation technique in a broad class of unbounded wave scattering problems [11, 32, 16] in a range of fields, including quantum mechanics, acoustics, electromagnetism (optics), and seismology. Mathematically, a PML can be equivalently understood as a complexified transformation of a coordinate [12]. A wave

*Received by the editors August 10, 2021; accepted for publication (in revised form) May 2, 2022; published electronically September 22, 2022.
https://doi.org/10.1137/21M1439705
Funding: The work of the second author was supported by the Alexander von Humboldt-Stiftung (AvH) Foundation during a visit to Karlsruhe Institute of Technology (KIT). The work of the third author was partially supported by the National Natural Science Foundation of China grant 12174310, the Natural Science Foundation of Zhejiang Province for Distinguished Young Scholars grant LR21A010001, and a Key Project of Joint Funds for Regional Innovation and Development (U21A20425).
†School of Mathematical Sciences, Zhejiang University, Hangzhou 310027, China (yuxiuchen@zju.edu.cn).
‡School of Mathematical Sciences and LPMC, Nankai University, Tianjin 100193, China (ghhu@nankai.edu.cn).
§Corresponding author. School of Mathematical Sciences, Zhejiang University, Hangzhou 310027, China (wangtaolu@zju.edu.cn).
¶Weierstrass Institute, Mohrenstr. 39, 10117 Berlin, Germany (Andreas.Rathsfeld@wias-berlin.de).

outgoing along the coordinate is then analytically continued in the complex plane and becomes exponentially decaying in the PML. However, such a double-edged feature causes the PML to be placed only in the direction where the medium structure is invariant so as to guarantee the validity of analytic continuation. Consequently, PML loses its prominence for some complicated structures, such as periodic structures [21]. Motivated by this, in this paper we study wave scattering in a half space of a homogeneous medium bounded by a two-dimensional (2D), perfectly conducting, and locally defected periodic surface, and we investigate the potential of PML in designing an accurate boundary integral equation (BIE) solver for the scattering problem.

Let a cylindrical wave due to a line source, or a downgoing plane wave, be specified above the defected surface. Then, a primary question is to understand clearly how the scattered wave radiates at infinity. Intrinsically, PML is closely related to the well-known Sommerfeld radiation condition (SRC), which, arguably, is an alternative way of saying "*wave is purely outgoing at infinity*." However, SRC is considered to be no longer valid for characterizing the scattered wave even when the surface is flat [2]. Instead, the upward propagation radiation condition (UPRC), a.k.a. the angular spectrum representation condition [14], is commonly used and can well pose the present problem or even more general rough surface scattering problems [5, 7, 8]. Milder than SRC, UPRC only requires that the scattered wave contain no downgoing waves on top of a straight line above the surface, allowing waves that are incoming horizontally from infinity.

If the surface has no defects, the total wave field for the plane-wave incidence is quasi-periodic so that the original scattering problem can be formulated in a single unit cell, bounded laterally but unbounded vertically. According to UPRC, the scattered wave at infinity can then be expressed in terms of upgoing Bloch waves, so that a transparent boundary condition or PML of a local/nonlocal boundary condition can be successfully used to terminate the unit cell vertically; the reader is referred to [3, 10, 26, 35] and the references therein for related numerical methods as well as theories of exponential convergence due to a PML truncation. But for the case when the incident wave is non–quasi-periodic, e.g., the cylindrical wave, or if the surface is locally defected, much fewer numerical methods or theories have been developed, as it is no longer straightforward to laterally terminate the scattering domain. Existing laterally truncating techniques include the recursive doubling procedure (RDP) [34, 15], Floquet–Bloch mode expansion [17, 20, 24], and the Riccati-equation based exact boundary condition [22].

In a recent work [19], we proved that the total field for the cylindrical incidence, a.k.a. the Green function, satisfies the standard SRC on top of a straight line above the surface. Based on this, we further revealed that for the plane-wave incidence, the perturbed part of the total field due to the defect satisfies the SRC as well. Consequently, this suggests using a PML to terminate the vertical variable so as to truncate the unbounded domain onto a strip, which is bounded vertically but unbounded laterally. In fact, such a natural setup of a PML had already been adopted in the literature [34, 6, 33] but without a rigorous justification of the outgoing behavior. It is worthwhile to mention that Chandler-Wilde and Monk in [6] rigorously proved that under a Neumann-condition PML, the PML solution converges to the true solution in the whole physical region of the strip at the rate of only an algebraic order of PML thickness; they further revealed that the PML solution due to the cylindrical incidence for a flat surface decays exponentially at infinity of a rectangular strip. However, it remains unclear how the PML solution radiates at infinity of the more generally curved strip under consideration. On the other hand, no literally rigorous theory has

been developed to clearly understand why this PML-truncated strip can further be laterally truncated to a bounded domain by the aforementioned techniques without introducing artificial ill-posedness; in other words, the well-posedness of scattering problems in exterior regions of the truncated domain is unjustified.

To address these questions, we first prove in this paper that under a Dirichlet-condition PML, the PML solution due to the cylindrical incidence, i.e., the Green function of the strip, converges to the true solution in the physical subregion of the strip at an algebraic order of the PML thickness. Next, we split the strip into three regions: a bounded region containing the defect, and two semi-waveguide regions of a single-directional periodic surface, separated by two vertical line segments. By use of the Green function of the strip, transparent boundary conditions can be developed to truncate the unbounded semi-waveguides. Based on this, we apply the method of variational formulation and the Fredholm alternative to prove the well-posedness of the scattering problem in either semi-waveguide so as to define a Neumann-to-Dirichlet (NtD) operator on its associated vertical segment. The two NtD operators serve exactly as lateral boundary conditions to terminate the strip and to reformulate the unbounded strip problem as a boundary value problem on the defected region. Due to the periodicity of the semi-waveguides, both NtD operators turn out to be closely related to a Neumann-marching operator, which is a solution of a nonlinear Riccati equation. It is proved that the Neumann-marching operators are contracting, indicating that the PML solution decays exponentially fast along both lateral directions even for the curved strip. The consequences culminate in two opposite aspects. Positively, from a numerical perspective, the Riccati equations can be efficiently solved by an RDP method so that the strip can be laterally truncated with ease. Negatively, the PML solution shall never exponentially converge to the true solution in the whole physical region of the strip. Nevertheless, as conjectured in [6], exponential convergence is optimistically expected to be realizable in any compact subdomain of the strip.

To validate the above conjecture numerically, we employ a high-accuracy PML-based boundary integral equation (BIE) method [29] to execute the RDP so that the two Riccati equations can be accurately solved for the two Neumann-marching operators, respectively, and hence the two NtD operators terminating the strip can be obtained. With the two NtD operators well prepared, the boundary value problem in the defected region can be accurately solved by the PML-based BIE method again. By carrying out several numerical experiments, we observe that the PML truncation error for the wave field over the defected part of the surface decays exponentially fast as PML absorbing strength or thickness increases. This indicates that there is a chance that the PML solution still converges to the true solution exponentially in any compact subdomain of the strip, the justification of which remains open.

The rest of this paper is organized as follows. In section 2, we introduce the half-space scattering problem and present some known well-posedness results. In section 3, we introduce a Dirichlet-condition PML, prove the well-posedness of the PML-truncated problem, and study the prior error estimate of the PML truncation. In section 4, we study well-posedness of the semi-waveguide problems. In section 5, we establish lateral boundary conditions, prove the exponentially decaying property of the PML solution at infinity of the strip, and develop an RDP technique to get the lateral boundary conditions. In section 6, we present a PML-based BIE method to numerically solve the scattering problem. In section 7, numerical experiments are carried out to demonstrate the performance of the proposed numerical method and to validate the proposed theory. We draw our conclusion finally in section 8 and propose

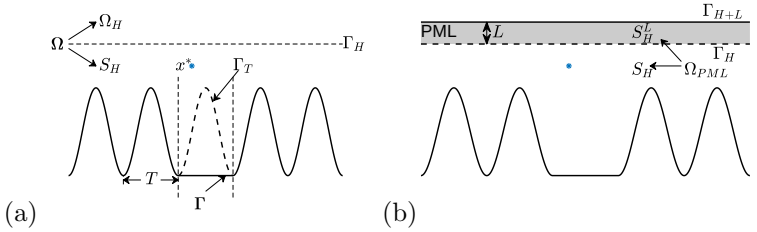

FIG. 1. (a) *A sketch of the half-space scattering problem.* (b) *A PML placed above* Γ. *The scattering surface* Γ *locally perturbs the periodic curve* Γ_T *of period* T. x^* *represents the exciting source.* Γ_H *is an artificial interface, on which a DtN map is defined or a PML is placed.*

some future plans.

2. Problem formulation. Let $\Omega \times \mathbb{R} \subset \mathbb{R}^3$ be an x_3-invariant domain bounded by a perfectly conducting surface $\Gamma \times \mathbb{R}$, where $\Gamma \subset \mathbb{R}^2$, bounding domain $\Omega \subset \mathbb{R}^2$, is a local perturbation of a T-periodic curve $\Gamma_T \subset \mathbb{R}^2$ periodic in the x_1-direction, as shown in Figure 1(a). We denote the Cartesian coordinate system of $\mathbb{R}^3$ by (x_1, x_2, x_3) and let $x = (x_1, x_2) \in \Omega$. Throughout this paper, we shall assume that Γ is Lipschitz and that Ω satisfies the following geometrical condition:

$$(x_1, x_2) \in \Omega \Rightarrow (x_1, x_2 + a) \in \Omega \quad \forall a \geq 0. \tag{GC}$$

For simplicity, suppose Γ only perturbs one periodic part of Γ_T, say $|x_1| < \frac{T}{2}$.

Let the unbounded domain $\Omega \times \mathbb{R}$ be filled by a homogeneous medium of refractive index n. For a time-harmonic, transverse-electric (TE), polarized electromagnetic wave excited by an x_3-invariant incoming field of time dependence $e^{-\mathbf{i}\omega t}$ with angular frequency ω, the x_3-component of the electric field, denoted by u^{tot}, is x_3-invariant, has the same time dependence, and satisfies the following boundary value problem for the 2D Helmholtz equation

$$\Delta u^{\text{tot}} + k^2 u^{\text{tot}} = 0 \quad \text{in} \quad \Omega, \tag{1}$$

$$u^{\text{tot}} = 0 \quad \text{on} \quad \Gamma, \tag{2}$$

where $\Delta = \partial_{x_1}^2 + \partial_{x_2}^2$ is the 2D Laplacian, and $k = k_0 n$ with $k_0 = \frac{2\pi}{\lambda}$ denoting the free-space wavenumber for wavelength λ.

Let an incident wave u^{inc} be specified in Ω, and let $x = (x_1, x_2) \in \Omega$. In this paper, we shall mainly focus on the following two cases of incidences: (i) a plane wave $u^{\text{inc}}(x) = e^{\mathbf{i}k(\cos\theta x_1 - \sin\theta x_2)}$ for the incident angle $\theta \in (0, \pi)$; (ii) a cylindrical wave $u^{\text{inc}}(x; x^*) = G(x; x^*) = \frac{\mathbf{i}}{4} H_0^{(1)}(k|x - x^*|)$ excited by a source at $x^* = (x_1^*, x_2^*) \in \Omega$. In the latter case, equation (1) should be replaced by

$$\Delta u^{\text{tot}} + k^2 u^{\text{tot}} = -\delta(x - x^*), \tag{3}$$

so that $u^{\text{tot}}(x; x^*)$ in fact represents the Green function excited by the source point x^*. For simplicity, we assume that $|x_1^*| < T/2$ so that x^* is right above the perturbed part of Γ.

Let $u^{\text{sc}} = u^{\text{tot}} - u^{\text{inc}}$ denote the scattered wave. One may enforce the following UPRC:

$$u^{\text{sc}}(x) = 2 \int_{\Gamma_H} \frac{\partial G(x; y)}{\partial y_2} u^{\text{sc}}(y) ds(y), \tag{4}$$

where $\Gamma_H = \{(x_1, H) : x_1 \in \mathbb{R}\}$ denotes a straight line strictly above Γ for some $H > 0$ and $y = (y_1, y_2)$. According to [7], the UPRC helps to define a Dirichlet-to-Neumann (DtN) map $\mathcal{T} : H^{1/2}(\Gamma_H) \to H^{-1/2}(\Gamma_H)$ for the domain $\Omega_H = \{x \in \Omega : x_2 > H\}$, such that for any $\phi \in H^{1/2}(\Gamma_H)$,

$$\mathcal{T}\phi = \mathcal{F}^{-1} M_z \hat{\phi}, \tag{5}$$

where $\hat{\phi}(H;\xi) = [\mathcal{F}\phi](H;\xi)$ denotes the normalized Fourier transform

$$[\mathcal{F}\phi](H;\xi) = \frac{1}{\sqrt{2\pi}} \int_{\mathbb{R}} \phi(x_1, H) e^{-\mathbf{i}\xi x_1} dx_1, \tag{6}$$

and the operator M_z in the space of Fourier transforms is the operator of multiplication by

$$z(\xi) = \begin{cases} -\mathbf{i}\sqrt{k^2 - \xi^2} & \text{for } |\xi| \le k, \\ \sqrt{\xi^2 - k^2} & \text{for } |\xi| > k. \end{cases} \tag{7}$$

Then, we may enforce

$$\partial_\nu u^{\mathrm{sc}} = -\mathcal{T} u^{\mathrm{sc}} \quad \text{on} \quad \Gamma_H, \tag{8}$$

where, unless otherwise indicated, ν always denotes the outer unit normal vector on Γ_H. The UPRC guarantees the well-posedness of our scattering problem [7] but does not force u^{sc} to be purely outgoing at infinity, largely limiting its applications in designing numerical algorithms.

Nevertheless, our recent work [19] has shown a stronger Sommerfeld-type condition for the aforementioned two incidences, which still preserves the well-posedness. Note that [19] assumes that each period of Γ_T contains a line segment, which guarantees a special local behavior of the Green function $u^{\mathrm{tot}}(x;y)$ for any x, y sufficiently close to each line segment. Such a technical assumption can be removed by constructing the DtN operator based on the idea of [18]. We will sketch this idea in the proof of Theorem 4.1 below. Let $S_H = \Omega \cap \{x : x_2 < H\}$ be the strip between Γ_H and Γ. The radiation condition reads as follows:

(i) In the case of plane-wave incidence, the outgoing wave is $u^{\mathrm{og}} := u^{\mathrm{tot}} - u^{\mathrm{tot}}_{\mathrm{ref}}$, where $u^{\mathrm{tot}}_{\mathrm{ref}}$ is the reference scattered field for the unperturbed scattering curve $\Gamma = \Gamma_T$, and satisfies the following half-plane Sommerfeld radiation condition (hSRC): For a sufficiently large $R > 0$ and any $\rho < 0$,

$$\begin{gathered} \lim_{r\to\infty} \sup_{\alpha\in[0,\pi]} \sqrt{r}\,|\partial_r u^{\mathrm{og}}(x) - \mathbf{i}k u^{\mathrm{og}}(x)| = 0, \\ \sup_{r\ge R} r^{1/2} |u^{\mathrm{og}}(x)| < \infty, \\ \text{and } u^{\mathrm{og}} \in H^1_\rho(S^R_H), \end{gathered} \tag{9}$$

where $x = (r\cos\alpha, H + r\sin\alpha)$, $S^R_H = S_H \cap \{x : |x_1| > R\}$, and $H^1_\rho(\cdot) = (1 + x_1^2)^{-\rho/2} H^1(\cdot)$ denotes a weighted Sobolev space. We defer the computation of $u^{\mathrm{tot}}_{\mathrm{ref}}$ to section 6.3.

(ii) For the cylindrical incidence, the total field is the outgoing wave $u^{\mathrm{og}} := u^{\mathrm{tot}}$ and satisfies the hSRC (9) in Ω_H. Thus, the scattered field u^{sc} satisfies (9) as well since u^{inc} satisfies (9).

Certainly, u^{og} satisfies the UPRC condition (4) such that (8) holds for u^{og} in place of u^{sc} [9, Thm. 2.9(ii)].

We recall some important results from [7]. For the cylindrical incident wave $u^{\text{inc}}(x;x^*)$, to remove the singularity of the right-hand side of (3), let

$$u_r^{\text{og}}(x;x^*) = u^{\text{og}}(x;x^*) - \chi(x;x^*)u^{\text{inc}}(x;x^*), \tag{10}$$

where the cut-off function $\chi(x;x^*) = 1$ in a neighborhood of x^* and has a sufficiently small support enclosing x^*. Let $V_H = \{\phi|_{S_H} : \phi \in H_0^1(\Omega)\}$. Then, it is equivalent to seek $u_r^{\text{og}} \in V_H$ that satisfies the boundary value problem

$$\Delta u_r^{\text{og}} + k^2 u_r^{\text{og}} = g \qquad \text{in} \quad S_H, \tag{11}$$

$$\partial_\nu u_r^{\text{og}} = -\mathcal{T} u_r^{\text{og}} \quad \text{on} \quad \Gamma_H, \tag{12}$$

where $g = -[\Delta\chi]u^{\text{inc}} - 2\sum_{j=1}^{2} \partial_{x_j}\chi\partial_{x_j}u^{\text{inc}} \in L^2(S_H)$ such that supp g is in the neighborhood of x^* contained in $\overline{S_H}$. An equivalent variational formulation reads as follows: Find $u_r^{\text{og}} \in V_H$ such that, for any $\phi \in V_H$,

$$b(u_r^{\text{og}}, \phi) = -(g, \phi)_{S_H}, \tag{13}$$

where the sesquilinear form $b(\cdot,\cdot) : V_H \times V_H \to \mathbb{C}$ is given by

$$b(\phi,\psi) = \int_{S_H} (\nabla\phi \cdot \nabla\bar{\psi} - k^2\phi\bar{\psi})dx + \int_{\Gamma_H} \mathcal{T}\phi\bar{\psi}ds. \tag{14}$$

For the incident plane wave $u^{\text{inc}}(x)$, the trace of $u_{\text{ref}}^{\text{tot}}$ on Γ, denoted by g_{ref}, belongs to $H^{1/2}(\Gamma)$, with $\overline{\Gamma\backslash\Gamma_T}$ being its support. Note that an extension of $u_{\text{ref}}^{\text{tot}}$ to a larger domain containing Γ is required if the perturbed curve Γ is not contained in the domain above the unperturbed periodic curve Γ_T. Then, following the proof of Theorem 4.10 in [31], one can also transform the original problem (1), (2) into the same problem (11), (12), where now

$$g = -(\Delta + k^2)[\chi_{\text{ref}}\, \eta\, g_{\text{ref}}] \in (H^1(S_H))^*,$$

$\eta\colon H^{1/2}(\Gamma\backslash\Gamma_T) \to H^1(S_H)$ denotes an extension operator, and χ_{ref} is a cut-off function with a small support containing $\overline{\Gamma\backslash\Gamma_T}$ so that $g \in V_H^*$. Due to the similarity between the two incidences, we shall only consider the theoretical details for the cylindrical incidence. However, in section 6.3, we shall discuss how to compute u^{tot} for a plane-wave incidence numerically.

It has been shown in [7] that b satisfies the following inf-sup condition: For all $v \in V_H$,

$$\gamma||v||_{V_H} \le \sup_{\phi\in V_H} \frac{|b(v,\phi)|}{||\phi||_{V_H}}, \tag{15}$$

where $\gamma > 0$ depends on H, k, and Ω. Furthermore, b defines an invertible operator $\mathcal{A} : V_H \to V_H^*$ such that $(\mathcal{A}\phi,\psi) = b(\phi,\psi)$ and $||\mathcal{A}^{-1}|| \le \gamma^{-1}$. Thus, $u_r^{\text{og}} = -\mathcal{A}^{-1}g$ so that $u^{\text{og}} = -\mathcal{A}^{-1}g + \chi u^{\text{inc}}$ for the cylindrical incident wave u^{inc}.

The hSRC (9) suggests computing the outgoing wave u^{og} numerically, as the PML technique [4, 6] could apply now to truncate the x_2-direction. In the following sections, we shall first introduce the setup of a PML to truncate x_2 and then develop an accurate lateral boundary condition to truncate x_1.

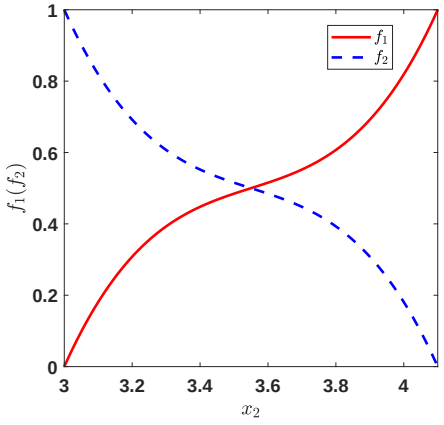

FIG. 2. *The two functions f_1 and f_2 for $m = 6$, $H = 3$, and $L = 2.2$.*

3. PML truncation. Mathematically, the PML truncating x_2 introduces a complexified coordinate transformation

$$\tilde{x}_2 = x_2 + \mathbf{i}S \int_0^{x_2} \sigma(t)dt, \tag{16}$$

where $\sigma(x_2) = 0$ for $x_2 \le H$ and $\sigma(x_2) \ge 0$ for $x_2 \ge H$; note that such a tilde notation can also be used to define $\tilde{y}_2$ and $\tilde{x}_2^*$ in the following. As shown in Figure 1(b), the planar strip $S_H^L = \mathbb{R} \times [H, H + L]$ with nonzero σ is called the PML region so that L represents its thickness. In this paper, we choose an $m \ge 0$ and

$$\sigma(x_2) = \begin{cases} \frac{2f_2^m}{f_1^m + f_2^m}, & x_2 \in [H, H + L/2], \\ 2, & x_2 \ge H + L/2, m \ne 0, \\ 1, & x_2 \ge H + L/2, m = 0, \end{cases} \tag{17}$$

where we note that $\sigma \equiv 1$ if $m = 0$, and

$$f_1 = \left(\frac{1}{2} - \frac{1}{m}\right)\xi^3 + \frac{\xi}{m} + \frac{1}{2}, \quad f_2 = 1 - f_1, \quad \xi = \frac{2x_2 - (2H + L/2)}{L/2}.$$

Let $L_c := \tilde{x}_2(H + L) - H = L + \mathbf{i}S_c L$, where $S_c = \frac{S}{L}\int_H^{H+L} \sigma(t)dt \ge S$. Both the real and imaginary parts of L_c affect the absorbing strength of the PML [12]. For $m = 6$, $H = 3$, and $L = 2.2$, we show the pictures of f_1 and f_2 for $x_2 \in [3, 4.2]$ in Figure 2.

Now, let $\tilde{x} = (x_1, \tilde{x}_2)$. For $x^* \in \Omega$ with $x_2 > H$, by analytic continuation of (4) we can define

$$u^{\mathrm{og}}(\tilde{x}; x^*) := 2\int_{\Gamma_H} \frac{\partial G(\tilde{x}; y)}{\partial y_2} u^{\mathrm{og}}(y; x^*)ds(y),$$

satisfying

$$\tilde{\Delta}u^{\mathrm{og}}(\tilde{x}; x^*) + k^2 u^{\mathrm{og}}(\tilde{x}; x^*) = -\delta(x - x^*),$$

where $\tilde{\Delta} = \partial_{x_1}^2 + \partial_{\tilde{x}_2}^2$. By the chain rule, we see that $\tilde{u}^{\mathrm{og}}(x; x^*) := u^{\mathrm{og}}(\tilde{x}; x^*)$ satisfies

$$\nabla \cdot (\mathbf{A}\nabla \tilde{u}^{\mathrm{og}}) + k^2 \alpha \tilde{u}^{\mathrm{og}} = -\delta(x - x^*) \quad \text{in } \Omega_{\mathrm{PML}}, \tag{18}$$

$$\tilde{u}^{\mathrm{og}} = 0 \quad \text{on} \quad \Gamma, \tag{19}$$

where $\mathbf{A} = \mathrm{diag}\{\alpha(x_2), 1/\alpha(x_2)\}$, $\alpha(x_2) = 1 + \mathbf{i}S\sigma(x_2)$, and the PML region $\Omega_{\mathrm{PML}} = \Omega \cap \{x : x_2 \le H + L\}$ consists of the physical region S_H and the PML region S_H^L. On the PML boundary $x_2 = H + L$, we use the homogeneous Dirichlet boundary condition

$$\tilde{u}^{\mathrm{og}} = 0 \quad \text{on} \quad \Gamma_{H+L} = \{x : x_2 = H + L\}. \tag{20}$$

The authors in [6] adopted a Neumann condition on the PML boundary Γ_{H+L} and proved the well-posedness of the related PML truncation problem. Here, we choose the Dirichlet condition (20) since, as we shall see, our numerical results indicate that the Dirichlet-PML seems more stable than the Neumann-PML. Furthermore, we need the Green function of the strip $\tilde{u}^{\mathrm{og}}(x; x^*)$ for any $x^* \in \Omega_{\mathrm{PML}}$ and not only for $x^* \in S_H$ to establish lateral boundary conditions. For completeness, following the idea of [6] we shall study the well-posedness of the problem (18)–(20) for any $x^* \in \Omega_{\mathrm{PML}}$.

The fundamental solution of the anisotropic Helmholtz equation (18) is (see [29])

$$\tilde{G}(x; y) = G(\tilde{x}; \tilde{y}) = \frac{\mathbf{i}}{4} H_0^{(1)}[k\rho(\tilde{x}; \tilde{y})], \tag{21}$$

where $\tilde{y} = (y_1, \tilde{y}_2)$; the complexified distance function ρ is defined to be

$$\rho(\tilde{x}, \tilde{y}) = [(x_1 - y_1)^2 + (\tilde{x}_2 - \tilde{y}_2)^2]^{1/2}; \tag{22}$$

and the half-power operator $z^{1/2}$ is chosen to be the branch of $\sqrt{z}$ with nonnegative real part for $z \in \mathbb{C}\backslash(-\infty, 0]$ such that $\arg(z^{1/2}) \in [0, \pi)$. The special choice of σ in (17) ensures that

$$\tilde{G}(x; y) = \tilde{G}(x; y_{\mathrm{imag}}), \tag{23}$$

for any $x \in \Gamma_{H+L}$, whenever $y = (y_1, y_2)$ and $y_{\mathrm{imag}} = (y_1, 2(H + L) - y_2)$, the mirror image of y w.r.t. the line Γ_{H+L}, are sufficiently close to Γ_{H+L} so that $\rho(\tilde{x}; \tilde{y}) = \rho(\tilde{x}; \tilde{y}_{\mathrm{imag}})$.

To remove the singularity of the right-hand side of (18), we introduce

$$\tilde{u}_r^{\mathrm{og}}(x; x^*) = \tilde{u}^{\mathrm{og}}(x; x^*) - \chi(x; x^*)\tilde{u}^{\mathrm{inc}}(x; x^*), \tag{24}$$

with the same cut-off function χ as in (10), where $\tilde{u}^{\mathrm{inc}}(x; x^*) = u^{\mathrm{inc}}(\tilde{x}; \tilde{x}^*)$. Then, $\tilde{u}_r^{\mathrm{og}}$ satisfies

$$\nabla \cdot (\mathbf{A}\nabla \tilde{u}_r^{\mathrm{og}}) + k^2 \alpha \tilde{u}_r^{\mathrm{og}} = \tilde{g}^{\mathrm{inc}} \quad \text{in} \quad \Omega_{\mathrm{PML}}, \tag{25}$$

$$\tilde{u}_r^{\mathrm{og}} = 0 \quad \text{on} \quad \Gamma, \tag{26}$$

$$\tilde{u}_r^{\mathrm{og}} = 0 \quad \text{on} \quad \Gamma_{H+L}, \tag{27}$$

where

$$\tilde{g}^{\mathrm{inc}} = [\nabla \cdot (\mathbf{A}\nabla) + k^2 \alpha](1 - \chi(x; x^*))\tilde{u}^{\mathrm{inc}}(x; x^*) \in L^2(\Omega_{\mathrm{PML}}) \tag{28}$$

with $\mathrm{supp}\ \tilde{g}^{\mathrm{inc}} \subset \overline{\Omega_{\mathrm{PML}}} = \overline{S_H} \cup \overline{S_H^L}$. Taking into account that x^* can be located in S_H^L, the support $\mathrm{supp}\ \tilde{g}^{\mathrm{inc}}$ may not completely lie in the physical domain S_H.

To establish a DtN map on Γ_H like (8), we need to study the following boundary value problem in the PML strip S_H^L: Given $q \in H^{1/2}(\Gamma_H)$, $s \in H^{1/2}(\Gamma_{H+L})$, and $\tilde{g}^{\rm inc}_{\rm PML} = \tilde{g}^{\rm inc}|_{S_H^L} \in L^2(S_H^L)$ with supp $\tilde{g}^{\rm inc}_{\rm PML} \subset \overline{S_H^L}$, find $v \in H^1(S_H^L)$ such that

$$\nabla \cdot (\mathbf{A}\nabla v) + k^2 \alpha v = \tilde{g}^{\rm inc}_{\rm PML} \quad \text{in} \quad S_H^L, \tag{29}$$

$$v = q \quad \text{on} \quad \Gamma_H, \tag{30}$$

$$v = s \quad \text{on} \quad \Gamma_{H+L}. \tag{31}$$

Let

$$v_0(x) = v(x) - v^{\rm inc}_{\rm PML}(x), \quad v^{\rm inc}_{\rm PML}(x) := \int_{S_H^L} [\tilde{G}(x;y) - \tilde{G}(x;y_{\rm imag})]\tilde{g}^{\rm inc}_{\rm PML}(y)dy, \tag{32}$$

where we recall that $y_{\rm imag}$ is the mirror image of y w.r.t. the line Γ_{L+H}. Thus, v_0 satisfies

$$\nabla \cdot (\mathbf{A}\nabla v_0) + k^2 \alpha v_0 = 0 \quad \text{in} \quad S_H^L, \tag{33}$$

$$v_0 = q_n \quad \text{on} \quad \Gamma_H, \tag{34}$$

$$v_0 = s_n \quad \text{on} \quad \Gamma_{H+L}, \tag{35}$$

where $q_n = q - v^{\rm inc}_{\rm PML}|_{\Gamma_H} \in H^{1/2}(\Gamma_H)$ and $s_n = s - v^{\rm inc}_{\rm PML}|_{\Gamma_{H+L}} \in H^{1/2}(\Gamma_{H+L})$.

By the method of separation of variables, we can explicitly express v_0 in terms of $\hat{s}_n(\xi) = [\mathcal{F}s_n](H+L;\xi)$ and $\hat{q}_n(\xi) = [\mathcal{F}q_n](H;\xi)$, i.e., the Fourier transforms of q_n and s_n w.r.t. the variable x_1, so that the PML-truncated problem (25)–(27) can be reformulated as an equivalent boundary value problem on the physical region S_H: Find $\tilde{u}_r^{\rm og} \in V_H$ that satisfies

$$\nabla \cdot (\mathbf{A}\nabla \tilde{u}_r^{\rm og}) + k^2 \alpha \tilde{u}_r^{\rm og} = \tilde{g}^{\rm inc}|_{S_H} \quad \text{in} \quad S_H, \tag{36}$$

$$\partial_\nu \tilde{u}_r^{\rm og} = -\mathcal{T}_p \tilde{u}_r^{\rm og}|_{\Gamma_H} + f_p \quad \text{on} \quad \Gamma_H, \tag{37}$$

where

$$f_p = \mathcal{N}_p(v^{\rm inc}_{\rm PML}|_{\Gamma_{H+L}}) + \mathcal{T}_p(v^{\rm inc}_{\rm PML}|_{\Gamma_H}) + \partial_\nu v^{\rm inc}_{\rm PML}|_{\Gamma_H} \in H^{-1/2}(\Gamma_H), \tag{38}$$

and the two bounded operators $\mathcal{T}_p : H^{1/2}(\Gamma_H) \to H^{-1/2}(\Gamma_H)$ and $\mathcal{N}_p : H^{1/2}(\Gamma_{H+L}) \to H^{-1/2}(\Gamma_H)$ are defined through

$$\mathcal{F}[\mathcal{T}_p q_n](H;\xi) = z\frac{\exp(zL_c) + \exp(-zL_c)}{\exp(zL_c) - \exp(-zL_c)}\hat{q}_n,$$

$$\mathcal{F}[\mathcal{N}_p s_n](H+L;\xi) = z\frac{-2}{\exp(zL_c) - \exp(-zL_c)}\hat{s}_n;$$

note that the above definitions allow $\xi \in \mathbb{R}$ now, since limits can be considered when $z = 0$. The associated variational formulation reads as follows: Find $\tilde{u}_r^{\rm og} \in V_H$, such that for any $\psi \in V_H$,

$$b_p(\tilde{u}_r^{\rm og}, \psi) = -\int_{S_H} \tilde{g}^{\rm inc}|_{S_H}\bar{\psi}dx + \int_{\Gamma_H} f_p\bar{\psi}ds, \tag{39}$$

where the sesquilinear form $b_p(\cdot,\cdot) : V_H \times V_H \to \mathbb{C}$ is given by

$$b_p(\phi,\psi) = \int_{S_H} (\nabla\phi \cdot \nabla\bar{\psi} - k^2\phi\bar{\psi})dx + \int_{\Gamma_H} \bar{\psi}\mathcal{T}_p\phi ds. \tag{40}$$

As in [6], we define the k-dependent norm

$$||\phi||^2_{H^s(\mathbb{R})} = \int_{\mathbb{R}} (k^2+\xi^2)^s |[\mathcal{F}\phi](\xi)|^2 d\xi$$

for $H^s(\mathbb{R})$. Then, the following lemma roughly characterizes the difference of $\mathcal{T}_p$ and $\mathcal{T}$.

LEMMA 3.1. *For any L with $kS_cL > 0$, we have*

$$||\mathcal{T} - \mathcal{T}_p|| \le \frac{1}{kS_cL} + \frac{2}{\sqrt{3}} \frac{\exp(-[2kL])}{[2kL]}. \tag{41}$$

Proof. The proof is similar to that of [6, Thm. 3.1]. We omit the details here. ∎

Clearly, the sesquilinear form b_p in (40) defines a bounded linear functional $\mathcal{A}_p : V_H \to V_H^*$ such that, for any $\phi \in V_H$,

$$((\mathcal{A}-\mathcal{A}_p)\phi, \psi) = b(\phi,\psi) - b_p(\phi,\psi) = \int_{\Gamma_H} \bar{\psi}(\mathcal{T}-\mathcal{T}_p)\phi ds.$$

Analogous to [6, sect. 3], we see immediately that

$$||\mathcal{A}-\mathcal{A}_p|| \le 2||\mathcal{T}-\mathcal{T}_p|| \le \frac{2}{kS_cL} + \frac{2}{\sqrt{3}} \frac{\exp(-[2kL])}{[2kL]}.$$

Consequently, since $\mathcal{A}$ is invertible, $\mathcal{A}_p$ has a bounded inverse provided that S_cL and L are sufficiently large. Since the right-hand side of (39) defines a bounded functional in V_H^*, we in fact have justified the following well-posedness result.

THEOREM 3.1. *Provided that L and S_cL (note $S_cL \ge SL$) are sufficiently large, the PML-truncated problem* (18)–(20) *admits a unique solution $\tilde{u}^{\rm og}(x;x^*) = \tilde{u}_r^{\rm og}(x;x^*) + \chi(x;x^*)\tilde{u}^{\rm inc}(x;x^*)$ with $\tilde{u}_r^{\rm og} \in H_0^1(\Omega_{\rm PML}) = \{\phi \in H^1(\Omega_{\rm PML}) : \phi|_{\Gamma\cup\Gamma_{H+L}} = 0\}$ for any $x^* \in \Omega_{\rm PML}$. Moreover, there holds the estimate $||\tilde{u}_r^{\rm og}(\cdot;x^*)||_{H^1(\Omega_{\rm PML})} \le C||\tilde{g}^{\rm inc}||_{L^2(\Omega_{\rm PML})}$, where $\tilde{g}^{\rm inc}$ is defined by* (28). *If $x^* \in S_H$, then*

$$||u^{\rm og}(\cdot;x^*) - \tilde{u}^{\rm og}(\cdot;x^*)||_{V_H} \le \frac{2}{\gamma \min\left\{[kS_cL], \sqrt{3}[2kL]\exp([2kL])\right\} - 2} ||u_r^{\rm og}(\cdot;x^*)||_{V_H}. \tag{42}$$

Proof. The proof is similar to that of [6, Cor. 3.4]. ∎

REMARK 3.1. *The well-posedness in Theorem* 3.1 *holds in general for any Lipschitz curve satisfying* (GC).

4. Semi-waveguide problems. Unlike the exponential convergence results in [10, 35], (42) indicates only a poor convergence of the PML method over S_H. However, we believe that exponential convergence can be realized in a compact subset of S_H, which is indeed true if Γ is flat [6]. Then the vertical PML truncation is efficient, and the next essential question is how to accurately truncate $\Omega_{\rm PML}$ in the lateral x_1-direction. To address this, as inspired by [22] and as illustrated in Figure 3(a), we shall consider the two semi-waveguide problems

$$(P^{\pm}) \qquad \begin{cases} \nabla\cdot(\mathbf{A}\nabla\tilde{u}) + k^2\alpha\tilde{u} = 0 \quad \text{in} \quad \Omega^{\pm}_{\rm PML} := \Omega_{\rm PML} \cap \left\{x : \pm x_1 > \frac{T}{2}\right\}, \\ \tilde{u} = 0 \quad \text{on} \quad \Gamma^{\pm} := \Gamma \cap \left\{x : \pm x_1 > \frac{T}{2}\right\}, \\ \tilde{u} = 0 \quad \text{on} \quad \Gamma^{\pm}_{L+H} := \Gamma_{L+H} \cap \left\{x : \pm x_1 > \frac{T}{2}\right\}, \\ \partial_{\nu_c}\tilde{u} = g^{\pm} \quad \text{on} \quad \Gamma_0^{\pm} := \Omega_{\rm PML} \cap \left\{x : x_1 = \pm\frac{T}{2}\right\} \end{cases}$$

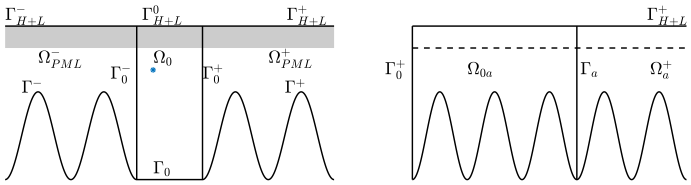

FIG. 3. (a) *Region* $\Omega_{\rm PML}$ *is divided into three regions* $\Omega^-_{\rm PML}$, Ω_0, *and* $\Omega^+_{\rm PML}$; *semi-waveguide problems* $(P^\pm)$ *are defined in* $\Omega^\pm$ *bounded by* $\Gamma^\pm_{H+L}$, $\Gamma^\pm_0$, *and* $\Gamma^\pm$. (b) *Domain* $\Omega^+_{\rm PML}$ *is further truncated onto* Ω_{0a} *by the curve* $\Gamma_a := \{x = (a, x_2) : x \in \Omega_{\rm PML}\}$ *for* $a \geq T/2$, *and* $\Omega^+_a = \Omega^+_{\rm PML} \backslash \overline{\Omega_{0a}}$.

for given Neumann data $g^\pm \in H^{-1/2}(\Gamma^\pm_0)$, where $\nu_c = \mathbf{A}\nu$ denotes the conormal vector with ν pointing toward $\Omega^\pm_{\rm PML}$, $\tilde{u}$ denotes a generic field, and we note that $\Gamma^\pm \subset \Gamma_T$ does not contain the defected part Γ_0. In this section, we shall study the well-posedness of the semi-waveguide problems $(P^\pm)$. We refer the reader to [31, Chap. 3] for the definition of Sobolev spaces $\tilde{H}^s(\Gamma^\pm_0)$ defined on the open arc $\Gamma^\pm_0$ and its dual space $H^{-s}(\Gamma^\pm_0)$ with $s \in \mathbb{R}$.

By Theorem 3.1, the following uniqueness result is easy to obtain.

LEMMA 4.1. *Provided that* $S_c L$ *and* L *are sufficiently large, problem* $(P^\pm)$ *has at most one solution in* $H^1(\Omega^\pm_{\rm PML})$.

Proof. Suppose $\tilde{u} \in H^1(\Omega^+_{\rm PML})$ satisfies (P^+) with $g^+ = 0$. Let

$$\Omega^e_{\rm PML} = \{x \in \mathbb{R}^2 : (x_1, x_2) \in \Omega^+_{\rm PML} \text{ or } (T - x_1, x_2) \in \Omega^+_{\rm PML}\} \cup \Gamma^+_0,$$
$$\Gamma^e = \{x \in \mathbb{R}^2 : (x_1, x_2) \in \Gamma^+ \text{ or } (T - x_1, x_2) \in \Gamma^+ \text{ or } (T/2, x_2) \in \Gamma\}.$$

Then,

$$\tilde{u}^e(x_1, x_2) = \begin{cases} \tilde{u}(x_1, x_2), & x_1 \geq T/2, \\ \tilde{u}(T - x_1, x_2), & x_1 < T/2, \end{cases}$$

in $H^1(\Omega^e_{\rm PML})$ satisfies problem (25)–(27) with $\tilde{g}$, $\Omega_{\rm PML}$, and Γ replaced by 0, $\Omega^e_{\rm PML}$, and Γ^e, respectively. Theorem 3.1 and Remark 3.1 imply that $\tilde{u}^e = 0$ on $\Omega^e_{\rm PML}$ so that $\tilde{u} = \tilde{u}^e|_{\Omega^+_{\rm PML}} = 0$. The uniqueness of problem (P^-) can be established similarly. ∎

In order to study the well-posedness of problem $(P^\pm)$ by Fredholm's alternative, we have to truncate $\Omega^+_{\rm PML}$ by imposing an exact transparent boundary condition, i.e., a condition including the DtN operator on an artificial boundary $\Gamma_a := \{x = (a, x_2) : x \in \Omega_{\rm PML}\}$ for some $a \geq T/2$. Let Ω^+_a be the unbounded domain bounded by Γ_a, Γ^+_{H+L}, and Γ, and as indicated in Figure 3(b), let Ω_{0a} be the domain bounded by Γ^+_0, Γ_a, Γ^+_{H+L}, and Γ_+. We suppose, without loss of generality, that both Ω^+_a and Ω_{0a} are Lipschitz domains. Otherwise, we can replace the segment Γ_a by a curve of a slightly different shape. To get the DtN operator over Γ_a without the technical assumption on Γ made in [19, section 2.3], we shall follow the ideas of [18]. The authors of [18] investigate well-posedness of time-harmonic electromagnetic scattering by perfectly conducting periodic surfaces with local perturbations in both TE and TM (transverse magnetic) polarizations. In a truncated bounded Lipschitz domain enclosing the perturbation, it is impossible in general to get an explicit form of the DtN map in the form of a series on the artificial boundary. In [18], the DtN operator is defined through the Green formula and extension operators, and a single layer operator is used to represent the wave fields in the exterior of the truncated

domain. For the purpose of avoiding the explicit use of the Green function, the single layer operator is defined as a well-defined transmission problem for the Helmholtz equation. Such an approach also leads to mapping properties of the single layer operator and carries over to the waveguide problems $(P^{\pm})$.

We first construct the single layer operator $\mathcal{S}_a$ on the artificial boundary Γ_a as follows: Given $\varphi \in H^{-1/2}(\Gamma_a)$, consider the transmission problem of finding $v \in H_0^1(\Omega_{\mathrm{PML}})$ such that

(43)
$$\nabla \cdot (\mathbf{A}\nabla v) + k^2 \alpha v = 0 \quad \text{in} \quad \Omega^+_{\mathrm{PML}} \cup \left[\Omega_{\mathrm{PML}} \setminus \overline{\Omega^+_{\mathrm{PML}}}\right], \qquad \partial_1^+ v - \partial_1^- v = \varphi \quad \text{on} \quad \Gamma_a,$$

where $\partial_1 := \partial/\partial x_1$. Note that the normal direction $\nu = (1,0)$ at Γ_a points into Ω_a^+. In the PML layer S_H^L, the equations in (43) can be written in the same form as in (29),

$$\nabla \cdot (\mathbf{A}\nabla v) + k^2 \alpha v = \tilde{g}^{\mathrm{inc}}_{\mathrm{PML}} \quad \text{in} \quad S_H^L, \tag{44}$$

with $\tilde{g}^{\mathrm{inc}}_{\mathrm{PML}} \in X^*$, $X := \{u \in H^1(S_H^L) : u = 0 \text{ on } \Gamma_{H+L}\}$, defined by

$$\langle \tilde{g}^{\mathrm{inc}}_{\mathrm{PML}}, w \rangle := \int_{\Gamma_a \cap S_H^L} \varphi\, \overline{w}\, ds, \quad w \in X.$$

Using $\tilde{g}^{\mathrm{inc}}_{\mathrm{PML}}$, we again define the functions $v_0, v^{\mathrm{inc}}_{\mathrm{PML}} \in H^1(S_H^L)$ and $f_p \in H^{-1/2}(\Gamma_H)$ as in (32) and (38). The variational formulation for v reads as (see, e.g., (39))

$$b_p(v,\psi) = \int_{\Gamma_a \cap S_H} \varphi \overline{\psi} ds + \int_{\Gamma_H} f_p \overline{\psi}\, ds \qquad \forall \quad \psi \in V_H, \tag{45}$$

where the sesquilinear form b_p is defined as in (40). Analogously to the proof of Theorem 3.1, one can show the unique solvability of $v \in H_0^1(\Omega_{\mathrm{PML}})$ provided L and $S_c L$ are sufficiently large. Moreover, the mapping $H^{-1/2}(\Gamma_a) \ni \varphi \mapsto v \in H_0^1(\Omega_{\mathrm{PML}})$ is bounded. The single layer operator $\mathcal{S}_a : H^{-1/2}(\Gamma_a) \to \tilde{H}^{1/2}(\Gamma_a)$ is then defined by $\mathcal{S}_a\varphi := v|_{\Gamma_a}$, which is obviously a bounded operator.

Next, we show that $\mathcal{S}_a$ is invertible and strongly elliptic. In the special case $k = i$, the well-posedness of (43) simply follows from the Lax–Milgram lemma. Indeed, from the variational formulation

$$a(v,\psi) := \int_{\Omega_{\mathrm{PML}}} \left[\alpha(x_2)\partial_1 v \overline{\partial_1 \psi} + 1/\alpha(x_2)\partial_2 v \overline{\partial_2 \psi} + \alpha(x_2) v \overline{\psi}\right] dx = \int_{\Gamma_a} \varphi \overline{\psi}\, ds, \quad \psi \in H_0^1(\Omega_{\mathrm{PML}}), \tag{46}$$

we observe that the sesquilinear form a is strictly coercive over $H_0^1(\Omega_{\mathrm{PML}})$, that is,

$$\mathrm{Re}\, a(v,v) \geq c\, ||v||^2_{H^1(\Omega_{\mathrm{PML}})}, \qquad c > 0. \tag{47}$$

Moreover, the variational solution v belongs to

$$H^1_{(\tau)}(\Omega_{\mathrm{PML}}) := \{u \in H_0^1(\Omega_{\mathrm{PML}}) : e^{\tau|x|} u \in H^1(\Omega_{\mathrm{PML}})\}$$

for $\tau \in (0,1)$, and the mapping $\varphi \mapsto v$ is bounded from $H^{-1/2}(\Gamma_a)$ into $H^1_{(\tau)}(\Omega_{\mathrm{PML}})$ and even compact from $H^{-1/2}(\Gamma_a)$ into $L^2_{(\tau')}(\Omega_{\mathrm{PML}}) := \{u \in H_0^1(\Omega_{\mathrm{PML}}) : e^{\tau'|x|} u \in$

$L^2(\Omega_{\rm PML})\}$ with $\tau' < \tau$ (cf. [18, Thm. 3.1]). Denote the operator mapping $\varphi \mapsto \tilde{v}|_{\Gamma_a}$, where $\tilde{v} \in L^2_{(\tau')}(\Omega_{\rm PML})$ is a solution of (46), by $\mathcal{S}_a^{(i)}$. Then it follows that $(\mathcal{S}_a - \mathcal{S}_a^{(i)})\varphi = w|_{\Gamma_a}$, where $w \in H^1_0(\Omega_{\rm PML})$ is the solution to

$$\nabla \cdot (\mathbf{A}\nabla w) + k^2 \alpha w = (k^2 - 1)\alpha \tilde{v} \quad \text{in} \quad \Omega_{\rm PML}. \tag{48}$$

The unique solvability of w to (48), which again goes back to the proof of Theorem 3.1, yields the boundedness of the mapping $L^2_{(\tau')}(\Omega_{\rm PML}) \ni v \mapsto w \in \tilde{H}^{1/2}(\Gamma_a)$. This, together with the compactness of $\varphi \mapsto \tilde{v}$ from $H^{-1/2}(\Gamma_a) \to L^2_{(\tau')}(\Omega_{\rm PML})$, proves the compactness of $\mathcal{S}_a - \mathcal{S}_a^{(i)}$. In summary, the single layer operator $\mathcal{S}_a : H^{-1/2}(\Gamma_a) \to \tilde{H}^{1/2}(\Gamma_a)$ can be decomposed into the sum of a compact operator $\mathcal{S}_a - \mathcal{S}_a^{(i)}$ and a coercive operator $\mathcal{S}_a^{(i)}$. On the other hand, we observe that $\mathcal{S}_a\varphi = v|_{\Gamma_a} = 0$ implies that $v \equiv 0$ in $\Omega_{\rm PML} \cap \{x_1 \leqslant a\}$ (see the proof of Lemma 4.1) and thus $\varphi = \partial_\nu^+ v|_{\Gamma_a} - \partial_\nu^- v|_{\Gamma_a} = 0$. Hence, the single layer operator $\mathcal{S}_a$ is boundedly invertible.

The DtN operator $\mathcal{T}_a : \tilde{H}^{1/2}(\Gamma_a) \to H^{-1/2}(\Gamma_a)$ is defined by $\mathcal{T}_a g = \partial_1 u|_{\Gamma_a}$ where $u \in H^1(\Omega_a^+)$ is the unique solution to

$$\begin{aligned} &\nabla \cdot (\mathbf{A}\nabla u) + k^2 \alpha u = 0 \quad \text{in} \quad \Omega_a^+, \qquad u = g \quad \text{on} \quad \Gamma_a, \\ &u = 0 \quad \text{on} \quad \partial\Omega_a^+ \cap \{\Gamma \cup \Gamma_{H+L}\}. \end{aligned} \tag{49}$$

By definition of the single layer operator, we conclude that the solution u of (49) coincides with the unique solution $v \in H^1_0(\Omega_{\rm PML})$ to (43) with $\varphi := \mathcal{S}_a^{-1} g \in H^{-1/2}(\Gamma_a)$ in Ω_a^+. This implies that the DtN operator $\mathcal{T}_a$ is well defined and bounded. Moreover, defining Γ_b and Ω_b^+ for $b > a$ similarly to Γ_a and Ω_a^+, the operator $\mathcal{T}_a$ takes the explicit form

$$\langle \mathcal{T}_a g, \psi \rangle = \int_{\Omega_a^+ \setminus \overline{\Omega_b^+}} \left[\mathbf{A}\nabla u \cdot \nabla \overline{\tilde{\psi}} - k^2 \alpha(x_2) u \overline{\tilde{\psi}} \right] dx, \quad \psi \in \tilde{H}^{1/2}(\Gamma_a), \tag{50}$$

where $\tilde{\psi} \in \{v \in H^1(\Omega_a^+ \setminus \overline{\Omega_b^+}) : v = 0 \text{ on } (\Gamma_{H+L} \cup \Gamma) \cap \{x : a \leq x_1 \leq b\} \text{ and on } \Gamma_b\}$ denotes an extension of $\psi \in \tilde{H}^{1/2}(\Gamma_a)$ obtained by a fixed bounded operator of extension. We are now ready to establish the well-posedness of problems $(P^\pm)$.

THEOREM 4.1. *Under the geometrical condition* (GC)*, provided that L and $S_c L$ are sufficiently large, the semi-waveguide problem $(P^\pm)$ has a unique solution $\tilde{u} \in H^1(\Omega^\pm_{\rm PML})$. Moreover, there holds $||\tilde{u}||_{H^1(\Omega^\pm_{\rm PML})} \leq C||g^\pm||_{H^{-1/2}(\Gamma_0^\pm)}$ for any $g^\pm \in H^{-1/2}(\Gamma_0^\pm)$, where C is independent of $g^\pm$.*

Proof. We only consider the problem (P^+), because (P^-) can be treated in the same manner. By (50), the DtN operator $\mathcal{T}_a$ can be decomposed into the sum of a coercive operator and a compact operator. Indeed, using the same arguments in proving (47) and the compactness of $\mathcal{S}_a - \mathcal{S}_a^{(i)}$, one can show that the DtN operator $\mathcal{T}_a^{(i)}$ corresponding to $k = i$ is coercive and the difference $\mathcal{T}_a - \mathcal{T}_a^{(i)}$ is compact. This implies that the DtN operator $\mathcal{T}_a : \tilde{H}^{1/2}(\Gamma_a) \to H^{-1/2}(\Gamma_a)$ is a Fredholm operator with index zero. The injectivity of $\mathcal{T}_a$ follows from the uniqueness result of Lemma 4.1. Hence, by Fredholm's alternative, the inverse $\mathcal{T}_a^{-1} : H^{-1/2}(\Gamma_a) \to \tilde{H}^{1/2}(\Gamma_a)$ exists and is bounded, which is nothing else but the NtD operator.

To prove Theorem 4.1, we take $a = T/2$ and thus $\Gamma_a = \Gamma_0^+$. For $g^+ \in H^{-1/2}(\Gamma_0^+)$, we have $\varphi := \mathcal{T}_{T/2}^{-1}(g^+) \in \tilde{H}^{1/2}(\Gamma_0^+)$. By definition of the DtN operator there exists a unique $u \in H^1(\Omega^+_{\rm PML})$ such that $u = \varphi$, $\partial_1 u = g^+$ on Γ_0^+ with the estimate

$$||u||_{H^1(\Omega^+_{\rm PML})} \leq C\,||\varphi||_{\tilde{H}^{1/2}(\Gamma_0^+)} \leq C\,||g^+||_{H^{-1/2}(\Gamma_0^+)}, \quad C > 0, \tag{51}$$

which proves Theorem 4.1. ∎

REMARK 4.1. *Like Theorem* 3.1*, Theorem* 4.1 *also holds for any Lipschitz curves* $\Gamma^{\pm}$*, which are not necessarily periodic, satisfying the geometrical condition* (GC).

REMARK 4.2. *Suppose that both the unperturbed curve* Γ_T *and the perturbed curve* Γ *are Lipschitz graphs and fulfill the geometrical condition* (GC). *The forward scattering problem* (1), (2) *admits a unique solution* u^{og} *which satisfies the hSRC* (9) *in* Ω_H *for any* $H > \max\{x_2 : x \in \Gamma \cup \Gamma_T\}$ *(see section* 2 *for the definitions of* u^{og} *and hSRC). This can be proved by constructing a new form of DtN operator analogously to the operator* $\mathcal{T}_a$. *We refer the reader to* [18] *for the radiation condition and the uniqueness and existence results for nongraph Lipschitz curves in the presence of evanescent surface waves.*

5. Lateral boundary conditions. According to Theorem 3.1, $\partial_{\nu_c}\tilde{u}^{\mathrm{og}}(\cdot;x^*)|_{\Gamma_0^{\pm}} \in H^{-1/2}(\Gamma_0^{\pm})$ for any $x^* \in S_H$ with $|x_1^*| < T/2$. Thus, $\tilde{u} = \tilde{u}^{\mathrm{og}}(\cdot;x^*)|_{\Omega_{\mathrm{PML}}^{\pm}}$ satisfies $(P^{\pm})$ with $g^{\pm} = \partial_{\nu_c}\tilde{u}^{\mathrm{og}}(\cdot;x^*)|_{\Gamma_0^{\pm}}$ in the distributional sense, respectively. Theorem 4.1 then implies that we can define two vertical NtD (vNtD) operators $\mathcal{N}^{\pm} : H^{-1/2}(\Gamma_0^{\pm}) \to \widetilde{H}^{1/2}(\Gamma_0^{\pm})$ satisfying $\tilde{u}^{\mathrm{og}}|_{\Gamma_0^{\pm}} = \mathcal{N}^{\pm}\partial_{\nu_c}\tilde{u}^{\mathrm{og}}|_{\Gamma_0^{\pm}}$. Such transparent boundary conditions can serve as exact *lateral boundary conditions* to terminate the x_1-variable for the PML-truncated problem (18), (19). Consequently, the original unbounded problem (1), (2) equipped with the hSRC condition (9) can be truncated onto the perturbed cell $\Omega_0 := \Omega_{\mathrm{PML}} \cap \left\{x : |x_1| < \frac{T}{2}\right\}$ and reformulated as the following boundary value problem:

(BVP1)
$$\begin{cases} \nabla\cdot(\mathbf{A}\nabla\tilde{u}^{\mathrm{og}}) + k^2\alpha\tilde{u}^{\mathrm{og}} = -\delta(x-x^*) & \text{in } \Omega_0, \\ \tilde{u}^{\mathrm{og}} = 0 & \text{on } \Gamma_0 = \Gamma \cap \{x : |x_1| < T/2\}, \\ \tilde{u}^{\mathrm{og}} = 0 & \text{on } \Gamma_{H+L}^0 = \Gamma_{H+L} \cap \{x : |x_1| < T/2\}, \\ \tilde{u}^{\mathrm{og}} = \mathcal{N}^{\pm}\partial_{\nu_c}\tilde{u}^{\mathrm{og}} & \text{on } \Gamma_0^{\pm}. \end{cases}$$

Theorems 3.1 and 4.1 directly imply that (BVP1) admits the unique solution

$$\tilde{u}^{\mathrm{og}}(\cdot;x^*) = \tilde{u}_r^{\mathrm{og}}(\cdot;x^*)|_{\Omega_0} + \chi(\cdot;x^*)|_{\Omega_0}\tilde{u}^{\mathrm{inc}}(x;x^*)|_{\Omega_0},$$

with $\tilde{u}_r^{\mathrm{og}}$ as defined in Theorem 3.1. Nevertheless, it is challenging to get $\mathcal{N}^{\pm}$ by directly solving the unbounded problem $(P^{\pm})$ in practice. To overcome this difficulty, in this section we shall define two closely related Neumann-marching operators, derive the governing Riccati equations, and design an efficient RDP to accurately approximate $\mathcal{N}^{\pm}$.

5.1. Solution operators $\mathcal{S}^{\pm}$ and Neumann-marching operators $\mathcal{R}_p^{\pm}$. Now, let $\Gamma_j^{\pm} = \{(x_1 \pm jT, x_2) : x = (x_1, x_2) \in \Gamma_0^{\pm}\}$, $\Omega_{\mathrm{PML},j}^{\pm} = \{x \in \Omega_{\mathrm{PML}}^{\pm} : \pm x_1 > T/2 + (j-1)T\}$, and $\Omega_j^{\pm} = \Omega_{\mathrm{PML},j}^{\pm} \backslash \overline{\Omega_{\mathrm{PML},j+1}^{\pm}}$, for $j \in \mathbb{N}^*$, as illustrated in Figure 4(a) for the notation with superscript $+$.

As inspired by [22], the well-posedness of $(P^{\pm})$ well defines two bounded solution operators $\mathcal{S}^{\pm} : H^{-1/2}(\Gamma_0^{\pm}) \to H^1(\Omega_{\mathrm{PML}}^{\pm})$ such that $\tilde{u}^{\mathrm{og}}|_{\Omega_{\mathrm{PML}}^{\pm}} = \mathcal{S}^{\pm}(\partial_{\nu_c}\tilde{u}^{\mathrm{og}}|_{\Gamma_0^{\pm}})$, and two bounded Neumann-marching operators $\mathcal{R}_p^{\pm} : H^{-1/2}(\Gamma_0^{\pm}) \to H^{-1/2}(\Gamma_1^{\pm})$ such that $\partial_{\nu_c^{\pm}}\tilde{u}^{\mathrm{og}}|_{\Gamma_1^{\pm}} = \mathcal{R}_p^{\pm}(\partial_{\nu_c^{\pm}}\tilde{u}^{\mathrm{og}}|_{\Gamma_0^{\pm}})$, where $\nu_c^{\pm} = \mathbf{A}\nu^{\pm}$ with $\nu^{\pm} = (\pm 1, 0)^T$. We have the following properties of $\mathcal{R}_p^{\pm}$, which are analogous to [22, Thm. 3.1].

PROPOSITION 5.1. *Under the condition that* kS_cL *and* kL *are sufficiently large, we can choose* $\Gamma_0^{\pm}$ *intersecting* Γ *at a smooth point such that* $\mathcal{R}_p^{\pm}$ *are compact operators*

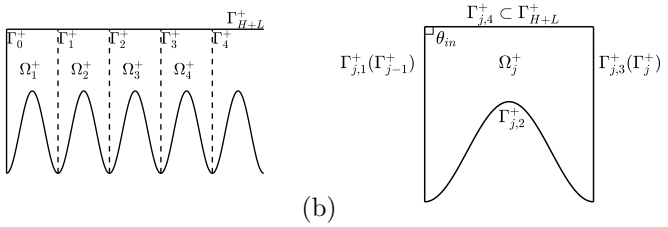

FIG. 4. (a) *The semi-waveguide region* $\Omega^+_{\rm PML}$ *is divided into domains* Ω^+_j, $j = 1, \ldots,$ *of the same shape. The operator* $\mathcal{R}^+_p$ *can then march Neumann data through the vertical line segments* Γ^+_j, $j = 0, \ldots$. (b) *The boundary of* Ω_j *consists of four parts:* $\Gamma^+_{j,1}$ *(left),* $\Gamma^+_{j,2}$ *(bottom),* $\Gamma^+_{j,3}$ *(right),* $\Gamma^+_{j,4}$ *(top). Here,* $\theta^{\rm in}$ *indicates the interior angle at a corner, as will be used in* (83).

and

$$\partial_{\nu_c^\pm}\tilde{u}^{\rm og}|_{\Gamma^\pm_{j+1}} = \mathcal{R}^\pm_p(\partial_{\nu_c^\pm}\tilde{u}^{\rm og}|_{\Gamma^\pm_j}) \tag{52}$$

holds for any $j \geq 0$. *Furthermore,*

$$\rho(\mathcal{R}^\pm_p) < 1, \tag{53}$$

where ρ *denotes the spectral radius.*

Proof. We study only the property of $\mathcal{R}^+_p$. The choice of Γ^+_0 and the interior regularity theory of elliptic operators directly imply the compactness of $\mathcal{R}^+_p$.

It is clear that (52) holds for $j = 0$. We need only justify the case $j = 1$, as all others can be done by induction. Consider the semi-waveguide problem (P^+) with $g^+ = -\partial_{\nu_c^+}\tilde{u}^{\rm og}|_{\Gamma^+_1}$, where the negative sign appears since $\nu_c^+ = -\nu_c$. Theorem 4.1 implies that $\tilde{u}^{\rm og}_n(x) = \tilde{u}^{\rm og}(x_1 + T, x_2)$ for $x \in \Omega^+_{\rm PML}$ is the unique solution. Then $\partial_{\nu_c^+}\tilde{u}^{\rm og}_n|_{\Gamma^+_1} = \mathcal{R}^+_p(\partial_{\nu_c^+}\tilde{u}^{\rm og}_n|_{\Gamma^+_0})$, which reads exactly as $\partial_{\nu_c^+}\tilde{u}^{\rm og}|_{\Gamma^+_2} = \mathcal{R}^+_p(\partial_{\nu_c^+}\tilde{u}^{\rm og}|_{\Gamma^+_1})$.

Now we prove (53) and take an arbitrary eigenfunction $0 \neq g \in H^{-1/2}(\Gamma^+_0)$ such that $\mathcal{R}^+_p g = \lambda_0 g$. Suppose $\tilde{u}$ satisfies (P^+) with $g^+ = g$ on Γ^+_0. Then, for any $v \in H^1(\Omega^+_{\rm PML})$, we get $v(\cdot - jT, \cdot) \in H^1(\Omega^+_{{\rm PML},j+1})$ for any $j \geq 0$, and, by the Green identity, that

$$\begin{aligned}
|\lambda_0|^j \left| \int_{\Gamma_0} g\bar{v} ds \right| &= \left| \int_{\Gamma_j} (\mathcal{R}^+_p)^j g \overline{v(\cdot - jT, \cdot)} ds \right| \\
&= \left| \int_{\Omega_{{\rm PML},j+1}} \left[(\mathbf{A}\nabla\tilde{u}^{\rm og})^T \overline{\nabla v(\cdot - jT, \cdot)} - k^2\alpha\tilde{u}^{\rm og}\overline{v(\cdot - jT, \cdot)} \right] dx \right| \\
&\leq C||\tilde{u}^{\rm og}||_{H^1(\Omega^+_{{\rm PML},j+1})}||v||_{H^1(\Omega^+_{\rm PML})} \to 0, \quad j \to \infty.
\end{aligned}$$

Choosing v such that $\int_{\Gamma_0} g\bar{v} ds \neq 0$, we get $|\lambda_0| < 1$, and (53) follows. ∎

By (53) and the identity (cf. [23])

$$\rho(\mathcal{R}^\pm_p) = \lim_{j\to\infty} ||(\mathcal{R}^\pm_p)^j||^{1/j},$$

there exists a sufficiently large integer $N_0 > 0$ such that $(\mathcal{R}^\pm_p)^{N_0}$ is contracting, i.e.,

$$||(\mathcal{R}^\pm_p)^{N_0}|| < 1. \tag{54}$$

Let $\Omega_j^{\pm,N_0}$ be the interior of N_0 consecutive cells $\cup_{j'=1}^{N_0}\overline{\Omega}^{\pm}_{(j-1)N_0+j'}$. As a corollary, the above results indicate that $\tilde{u}^{\rm og}$ decays exponentially at infinity of the strip.

COROLLARY 5.1. *Under the condition that kL and kS_cL are sufficiently large,*

$$||\tilde{u}^{\rm og}(\cdot;x^*)||_{H^1(\Omega_j^{\pm,N_0})} \le C||(\mathcal{R}_p^{\pm})^{N_0}||^{j-1}||\tilde{g}^{\rm inc}||_{L^2(\Omega_{\rm PML})}, \tag{55}$$

where we recall that $\tilde{g}^{\rm inc} = [\nabla\cdot(\mathbf{A}\nabla) + k^2\alpha](1-\chi(x;x^*))\tilde{u}^{\rm inc}(x;x^*)$, and C is independent of $j \ge 0$. In other words, for any $x^* \in \Omega_{\rm PML}$, the PML-truncated solution $\tilde{u}^{\rm og}(x;x^*)$ decays exponentially fast to 0 in the strip as $|x_1| \to \infty$.

REMARK 5.1. *The authors of* [6] *revealed a result similar to* (55) *for Γ being a flat surface. The above corollary indicates that such an exponentially decaying property for the PML-truncated solution holds even for locally defected periodic curves. As a consequence, this reveals that the PML truncation cannot realize an exponential convergence to the true solution for numerical solutions at regions sufficiently away from the source or local defects since the true solution is expected to decay only at an algebraic rate at infinity;* [7] *has indicated that $u^{\rm og}$ behaves as $\mathcal{O}(x_1^{-3/2})$ as $x_1 \to \infty$.*

Although, due to Corollary 5.1, an exponential convergence of the PML method in the whole physical domain S_H cannot be realized, it is the exponential decay property of $\tilde{u}^{\rm og}$ that makes the RDP, as introduced below, successful at effectively computing $\mathcal{R}_p^{\pm}$. Moreover, we point out that (55) holds for L being fixed but $j \to \infty$. If, on the contrary, j is fixed but $L \to \infty$, we believe exponential convergence can still be achieved. In doing so, we need a more effective description of the Neumann-marching operators $\mathcal{R}_p^{\pm}$, as was given in [22]. Take $\mathcal{R}_p^{+}$ as an example. As shown in Figure 4(b), Ω_j^+ denotes the jth unit cell on the right of Γ_0^+, which is unperturbed for $j \ge 1$, and to simplify the presentation, we further denote the four boundaries of Ω_j^+ by

$$\Gamma_{j,1} = \Gamma_{j-1}^+, \quad \Gamma_{j,3} = \Gamma_j^+, \quad \Gamma_{j,2} = \overline{\Omega_j^+} \cap \Gamma, \quad \Gamma_{j,4} = \overline{\Omega_j^+} \cap \Gamma_{H+L}^+.$$

Consider the following boundary value problem for a generic field $\tilde{u}$:

$$\text{(BVP2)} \qquad \begin{cases} \nabla\cdot(\mathbf{A}\nabla\tilde{u}) + k^2\alpha\tilde{u} = 0 & \text{in } \Omega_j^+, \\ \tilde{u} = 0 & \text{on } \Gamma_{j,2}\cup\Gamma_{j,4}, \\ \partial_{\nu_c}\tilde{u} = g_i & \text{on } \Gamma_i^+,\ i = j-1, j, \end{cases}$$

for $g_i \in H^{-1/2}(\Gamma_i^+),\ i = j-1, j$. We have the following well-posedness theorem.

THEOREM 5.1. *Provided that $kT/\pi \notin \mathcal{E} := \{i'/2^{j'} | j' \in \mathbb{N}, i' \in \mathbb{N}^*\}$, and that L, as well as S_cL, is sufficiently large,* (BVP2) *is well-posed. The well-posedness even holds with Ω_j^+ replaced by the interior domain of 2^l consecutive cells, say $\cup_{j=1}^{2^l}\overline{\Omega_j^+}$, for any number $l \ge 0$.*

Proof. It is clear that only uniqueness is needed [31, Thm. 4.10]. Suppose $j = 1$ and $g_i = 0,\ i = 0, 1$. Then, by first an even extension over Γ_0^+ and then a $2T$-periodic extension, we get a $2T$-periodic solution $\tilde{u}^e$ (corresponding to a normal incidence) in a strip bounded in the x_2-direction by a $2T$-periodic grating surface, possibly different from Γ, and the PML boundary Γ_{H+L}. However, according to the well-posedness theory [5, Cor. 5.2] for the half-space scattering by the grating, the PML convergence theory in [10, Thm. 2.4] can be readily adapted here to show that $\tilde{u}^e \equiv 0$, taking into account that $kT/\pi \notin \mathcal{E}$ has excluded horizontally propagating Bloch modes. ∎

REMARK 5.2. *We note that the condition $kT/\pi \notin \mathcal{E}$ is not necessary for the well-posedness of* (BVP2). *Alternatively, if $kT/\pi \in \mathcal{E}$, one may impose zero Neumann condition on $\Gamma_{4,j}$ to guarantee the uniqueness of the modified* (BVP2) [30, 35].

By Theorem 5.1, we can define a bounded NtD operator $\mathcal{N}^{(0)} : H^{-1/2}(\Gamma_{j-1}^+) \times H^{-1/2}(\Gamma_j^+) \to \widetilde{H}^{1/2}(\Gamma_{j-1}^+) \times \widetilde{H}^{1/2}(\Gamma_j^+)$ such that

$$\begin{bmatrix} \tilde{u}|_{\Gamma_{j-1}^+} \\ \tilde{u}|_{\Gamma_j^+} \end{bmatrix} = \mathcal{N}^{(0)} \begin{bmatrix} \partial_{\nu_c^-} \tilde{u}|_{\Gamma_{j-1}^+} \\ \partial_{\nu_c^+} \tilde{u}|_{\Gamma_j^+} \end{bmatrix} \tag{56}$$

for all $j \geq 1$. Due to the invariant shape of Ω_j^+ with respect to j, $\mathcal{N}^{(0)}$ is in fact independent of j. Suppose $j = 1$. Then, by the linearity principle, $\mathcal{N}^{(0)}$ can be rewritten in the matrix form

$$\mathcal{N}^{(0)} = \begin{bmatrix} \mathcal{N}_{00}^{(0)} & \mathcal{N}_{01}^{(0)} \\ \mathcal{N}_{10}^{(0)} & \mathcal{N}_{11}^{(0)} \end{bmatrix},$$

where the bounded map $\mathcal{N}_{i'j'}^{(0)} : H^{-1/2}(\Gamma_{j'}^+) \to \widetilde{H}^{1/2}(\Gamma_{i'})$ maps $\partial_{\nu_c} \tilde{u}|_{\Gamma_{j'}^+} = g_{j'}$ to $\tilde{u}|_{\Gamma_{i'}^+}$ if $g_{1-j'} = 0$ for $i', j' = 0, 1$ in (BVP2). Due to the shape invariance of Γ_j^+, we shall identify $H^{-1/2}(\Gamma_j^+)$ for all $j \geq 0$ as the same space $H^{-1/2}(\Gamma_0^+)$, and, similarly, the $\widetilde{H}^{1/2}(\Gamma_j^+)$ shall all be identified as the dual space of $H^{-1/2}(\Gamma_0^+)$.

Returning to the semi-waveguide problems $(P^{\pm})$, we have, by the definition of $\mathcal{R}_p^+$ and (56) for $j = 1$ and 2, that

$$\begin{aligned} &\mathcal{N}_{10}^{(0)} \partial_{\nu_c^-} \tilde{u}^{\mathrm{og}}|_{\Gamma_0^+} - \mathcal{N}_{11}^{(0)} \mathcal{R}_p^+ \partial_{\nu_c^-} \tilde{u}^{\mathrm{og}}|_{\Gamma_0^+} = \tilde{u}^{\mathrm{og}}|_{\Gamma_1^+} \\ &= \mathcal{N}_{00}^{(0)} \mathcal{R}_p^+ \partial_{\nu_c^-} \tilde{u}^{\mathrm{og}}|_{\Gamma_0^+} - \mathcal{N}_{01}^{(0)} (\mathcal{R}_p^+)^2 \partial_{\nu_c^-} \tilde{u}^{\mathrm{og}}|_{\Gamma_0^+}. \end{aligned} \tag{57}$$

Here and in the following, the product of two operators should be regarded as their composition. Thus,

$$\left[\mathcal{N}_{10}^{(0)} - \mathcal{N}_{11}^{(0)} \mathcal{R}_p^+ - \mathcal{N}_{00}^{(0)} \mathcal{R}_p^+ + \mathcal{N}_{01}^{(0)} (\mathcal{R}_p^+)^2 \right] \partial_{\nu_c} \tilde{u}^{\mathrm{og}}|_{\Gamma_0^+} = 0,$$

for any $\partial_{\nu_c} \tilde{u}^{\mathrm{og}}|_{\Gamma_0^+} \in H^{-1/2}(\Gamma_0^+)$, so that we end up with the following Riccati equation for $\mathcal{R}_p^+$:

$$\mathcal{N}_{10}^{(0)} - [\mathcal{N}_{11}^{(0)} + \mathcal{N}_{00}^{(0)}] \mathcal{R}_p^+ + \mathcal{N}_{01}^{(0)} (\mathcal{R}_p^+)^2 = 0. \tag{58}$$

One similarly obtains the governing equation for $\mathcal{R}_p^-$,

$$\mathcal{N}_{01}^{(0)} - [\mathcal{N}_{11}^{(0)} + \mathcal{N}_{00}^{(0)}] \mathcal{R}_p^- + \mathcal{N}_{10}^{(0)} (\mathcal{R}_p^-)^2 = 0. \tag{59}$$

Analogous to [22], the previous results in fact indicate that the two Riccati equations (58) and (59) must be uniquely solvable under the condition that $\rho(R_p^{\pm}) < 1$. The vNtD operators $\mathcal{N}^{\pm}$ mapping $\partial_{\nu_c} \tilde{u}^{\mathrm{og}}|_{\Gamma_0^{\pm}}$ to $\tilde{u}^{\mathrm{og}}|_{\Gamma_0^{\pm}}$ are, respectively, given by

$$\mathcal{N}^+ = \mathcal{N}_{00}^{(0)} - \mathcal{N}_{01}^{(0)} \mathcal{R}_p^+, \tag{60}$$

$$\mathcal{N}^- = \mathcal{N}_{11}^{(0)} - \mathcal{N}_{10}^{(0)} \mathcal{R}_p^-. \tag{61}$$

However, due to the nonlinearity of the Riccati equations (58) and (59), it is not that easy to get $\mathcal{N}^{\pm}$ in practice [22]. To tackle this difficulty, we shall develop an RDP to effectively approximate $\mathcal{R}_p^{\pm}$.

5.2. Recursive doubling procedure. Take $\mathcal{R}_p^+$ as an example. We first study the NtD operator

$$\mathcal{N}^{(l)} = \begin{bmatrix} \mathcal{N}_{00}^{(l)} & \mathcal{N}_{01}^{(l)} \\ \mathcal{N}_{10}^{(l)} & \mathcal{N}_{11}^{(l)} \end{bmatrix} \tag{62}$$

on the boundary of $\cup_{j=1}^{2^l}\overline{\Omega_j^+}$ for $l \geq 1$, where $\mathcal{N}_{i'j'}^{(l)}$ is bounded from $H^{-1/2}(\Gamma_0^+)$ to $\widetilde{H}^{1/2}(\Gamma_0)$ for $i', j' = 0, 1$. If $l = 1$, we need to compute $\mathcal{N}^{(1)}$ on the boundary of $\overline{\Omega_1^+ \cup \Omega_2^+}$. Using (56) for $j = 1$ and 2 and eliminating $\tilde{u}^{\rm og}$ and $\partial_{\nu_c}\tilde{u}^{\rm og}$ by the continuity condition on Γ_1^+, one gets

$$(\mathcal{N}_{00}^{(l-1)} + \mathcal{N}_{11}^{(l-1)})\partial_{\nu_c^+}\tilde{u}^{\rm og}|_{\Gamma_1^+} = -\mathcal{N}_{10}^{(l-1)}\partial_{\nu_c^-}\tilde{u}^{\rm og}|_{\Gamma_0^+} + \mathcal{N}_{01}^{(l-1)}\partial_{\nu_c^+}\tilde{u}^{\rm og}|_{\Gamma_2^+}. \tag{63}$$

By Theorem 5.1, the well-posedness of the modified (BVP2) for $l = 1$ indicates that there exist two bounded operators $\mathcal{A}_{l-1}, \mathcal{B}_{l-1} : H^{-1/2}(\Gamma_0^+) \to H^{-1/2}(\Gamma_0^+)$ such that

$$\partial_{\nu_c^+}\tilde{u}^{\rm og}|_{\Gamma_1^+} = -\mathcal{A}_{l-1}\partial_{\nu_c^-}\tilde{u}^{\rm og}|_{\Gamma_0^+} + \mathcal{B}_{l-1}\partial_{\nu_c^+}\tilde{u}^{\rm og}|_{\Gamma_2^+}.$$

Equation (63) implies that

$$\mathcal{A}_{l-1} = (\mathcal{N}_{00}^{(l-1)} + \mathcal{N}_{11}^{(l-1)})^{-1}\mathcal{N}_{10}^{(l-1)}, \quad \mathcal{B}_{l-1} = (\mathcal{N}_{00}^{(l-1)} + \mathcal{N}_{11}^{(l-1)})^{-1}\mathcal{N}_{01}^{(l-1)},$$

where $(\mathcal{N}_{00}^{(l-1)} + \mathcal{N}_{11}^{(l-1)})^{-1}$ is a generalized inverse from $\widetilde{H}^{1/2}(\Gamma_0)$ to $H^{-1/2}(\Gamma_0^+)$. Thus, one obtains

$$\mathcal{N}_{00}^{(l)} = \mathcal{N}_{00}^{(l-1)} - \mathcal{N}_{01}^{(l-1)}\mathcal{A}_{l-1}, \quad \mathcal{N}_{01}^{(l)} = \mathcal{N}_{01}^{(l-1)}\mathcal{B}_{l-1}, \tag{64}$$

$$\mathcal{N}_{10}^{(l)} = \mathcal{N}_{10}^{(l-1)}\mathcal{A}_{l-1}, \quad \mathcal{N}_{11}^{(l)} = \mathcal{N}_{11}^{(l-1)} - \mathcal{N}_{10}^{(l-1)}\mathcal{B}_{l-1}. \tag{65}$$

Equations (64)–(65) can be recursively applied to get $\mathcal{N}^{(l)}$ for all $l \geq 1$, and the number of consecutive cells $\{\Omega_j\}$ doubles after each iteration, which form the origin of the term *recursive doubling procedure* (RDP) in the literature [34, 15]. In the following, we shall see that RDP provides a simple approach for solving (58) and (59).

Now, analogously to (58) and (59), we obtain from $\mathcal{N}^{(l)}$ and (52) the following equations:

$$\mathcal{N}_{10}^{(l)} - [\mathcal{N}_{11}^{(l)} + \mathcal{N}_{00}^{(l)}](\mathcal{R}_p^+)^{2^l} + \mathcal{N}_{01}^{(l)}(\mathcal{R}_p^+)^{2^{(l+1)}} = 0, \tag{66}$$

$$\mathcal{N}^+ = \mathcal{N}_{00}^{(l)} - \mathcal{N}_{01}^{(l)}(\mathcal{R}_p^+)^{2^l}, \tag{67}$$

$$\mathcal{N}_{01}^{(l)} - [\mathcal{N}_{11}^{(l)} + \mathcal{N}_{00}^{(l)}](\mathcal{R}_p^-)^{2^l} + \mathcal{N}_{10}^{(l)}(\mathcal{R}_p^-)^{2^{(l+1)}} = 0, \tag{68}$$

$$\mathcal{N}^- = \mathcal{N}_{11}^{(l)} - \mathcal{N}_{10}^{(l)}(\mathcal{R}_p^-)^{2^l}. \tag{69}$$

We have the following convergence theorem.

THEOREM 5.2. *Provided that $kT/\pi \notin \mathcal{E}$, and that L, as well as S_cL, is sufficiently large, we have*

(70)
$$||\mathcal{N}_{10}^{(l)}|| \le C||(\mathcal{R}_p^+)^{2^l}||, \qquad ||\mathcal{N}_{01}^{(l)}|| \le C||(\mathcal{R}_p^-)^{2^l}||,$$

(71)
$$||\mathcal{N}^+ - \mathcal{N}_{00}^{(l)}|| \le C||(\mathcal{R}_p^+)^{2^l}|| \cdot ||(\mathcal{R}_p^-)^{2^l}||, \quad ||\mathcal{N}^- - \mathcal{N}_{11}^{(l)}|| \le C||(\mathcal{R}_p^+)^{2^l}|| \cdot ||(\mathcal{R}_p^-)^{2^l}||,$$

for any integer $l \ge l_0$, where the constant $C > 0$ depends only on $||\mathcal{N}^{\pm}||$ and $\rho(\mathcal{R}_p^{\pm})$. Moreover, for a fixed q with $\rho(\mathcal{R}_p^{\pm}) < q < 1$, the index l_0 is chosen such that $||(\mathcal{R}_p^{\pm})^{2^l}|| < q^{2^l}$ for any $l \ge l_0$.

Proof. The estimates (71) can be directly derived from (70), (67), and (69). In the following, we only prove the estimate for $\mathcal{N}_{10}^{(l)}$, and one can justify the estimate for $\mathcal{N}_{01}^{(l)}$ similarly. In the domain $\Omega^{(l)} = \cup_{j=1}^{2^l} \overline{\Omega_j^+}$, consider the boundary value problem

$$\begin{cases} \nabla \cdot (\mathbf{A}\nabla \tilde{u}) + k^2 \alpha \tilde{u} = 0 & \text{in } \Omega^{(l)}, \\ \tilde{u} = 0 & \text{on } (\Gamma^+ \cup \Gamma_{H+L}^+) \cap \overline{\Omega^{(l)}}, \\ \partial_{\nu_c} \tilde{u} = g & \text{on } \Gamma_0^+, \\ \partial_{\nu_c} \tilde{u} = 0 & \text{on } \Gamma_{2^l}^+ \end{cases}$$

for any $g \in H^{-1/2}(\Gamma_0^+)$. It is straightforward to verify that

$$\begin{aligned} \tilde{u} = & \left[\mathcal{S}^+ \left\{ \sum_{j=0}^{\infty} \left[(\mathcal{R}_p^-)^{2^l} (\mathcal{R}_p^+)^{2^l} \right]^j g \right\} \right] \Bigg|_{\Omega^{(l)}} \\ & - \left[\mathcal{S}^- \left\{ \sum_{j=0}^{\infty} \left[(\mathcal{R}_p^+)^{2^l} (\mathcal{R}_p^-)^{2^l} \right]^j (\mathcal{R}_p^+)^{2^l} g \right\} \right] (\cdot - (2^l+1)T, \cdot) \Bigg|_{\Omega^{(l)}} \end{aligned}$$

is a solution of the above problem and is unique by Theorem 5.1, where we recall that $\mathcal{S}^{\pm}$ are the two solution operators defined in section 5.1, and $(\cdot - (2^l+1)T, \cdot)$ indicates a translation in the x_1-direction such that for any $x = (x_1, x_2) \in \Gamma_{2^l}^+$, $(x_1 - (2^l+1)T, x_2) \in \Gamma_0^-$. The two series converge in $H^{-1/2}(\Gamma_0)$ since $||(\mathcal{R}_p^{\mp})^{2^l} (\mathcal{R}_p^{\pm})^{2^l}|| < 1$. Then

$$\begin{aligned} \mathcal{N}_{10}^{(l)} g = \tilde{u}|_{\Gamma_{2^l}^+} = & \mathcal{N}^+ \left\{ (R_p^+)^{2^l} \sum_{j=0}^{\infty} \left[(\mathcal{R}_p^-)^{2^l} (\mathcal{R}_p^+)^{2^l} \right]^j g \right\} \\ & - \mathcal{N}^- \left\{ \sum_{j=0}^{\infty} \left[(\mathcal{R}_p^+)^{2^l} (\mathcal{R}_p^-)^{2^l} \right]^j (\mathcal{R}_p^+)^{2^l} g \right\}. \end{aligned}$$

Obviously,

$$||\mathcal{N}_{10}^{(l)} g|| \le \left[\frac{||\mathcal{N}^+||}{1-q^2} + \frac{||\mathcal{N}^-||}{1-q^2} \right] ||(R_p^+)^{2^l}|| \cdot ||g||. \qquad \square$$

Theorem 5.2 indicates that we can directly approximate

$$\mathcal{N}^+ \approx \mathcal{N}_{00}^{(l)}, \quad \mathcal{N}^- \approx \mathcal{N}_{11}^{(l)}, \tag{72}$$

where the approximation errors decay exponentially as l increases. Moreover, for l sufficiently large, $||\mathcal{N}_{00}^{(l)}+\mathcal{N}_{11}^{(l)}|| = \mathcal{O}(1)$ and $||(\mathcal{N}_{00}^{(l)}+\mathcal{N}_{11}^{(l)})^{-1}|| = \mathcal{O}(1)$. The last assertion is a consequence of (71) and of the invertibility of $\mathcal{N}^+ + \mathcal{N}^- = \lim_{l\to\infty}[\mathcal{N}_{00}^{(l)} + \mathcal{N}_{11}^{(l)}]$. Indeed, for the invertibility of $\mathcal{N}^+ + \mathcal{N}^-$, we remark that $\mathcal{N}^\pm$ is strongly elliptic, which follows from the strong ellipticity of its inverse (e.g., $(\mathcal{N}^+)^{-1} = \mathcal{T}_a$) shown in the proof of Theorem 4.1. Hence, the strong ellipticity implies the Fredholm property with index zero for $\mathcal{N}^+ + \mathcal{N}^-$. On the other hand, for a function g with $[\mathcal{N}^+ + \mathcal{N}^-]g = 0$, we define $\tilde{u}_0$ over $\Omega^+_{\rm PML}$ as the solution $\tilde{u}$ of P^+ with $g^+ := g$ and over the shifted domain $S\Omega^-_{\rm PML} := \{(x_1, x_2)\colon (x_1 + T, x_2) \in \Omega^-_{\rm PML}\}$ by $\tilde{u}_0(x_1 + T, x_2) := \tilde{u}(x_1, x_2)$, where $\tilde{u}$ is the solution of P^- with $g^-(x_1, x_2) := -g(x_1 + T, x_2)$. Then $[\mathcal{N}^+ + \mathcal{N}^-]g = 0$ implies the continuity of $\tilde{u}_0$ and $\partial_2\tilde{u}_0$ through Γ_0^+, and the choice of the $g^\pm$ the continuity of $\partial_c\tilde{u}_0$. Consequently, $\tilde{u}_0$ is a solution of the homogeneous Dirichlet problem over the periodic unperturbed domain $\Omega^+_{\rm PML} \cup S\Omega^-_{\rm PML}$ such that the unique solvability of Theorem 3.1 provides $\tilde{u}_0 \equiv 0$ and $g \equiv 0$. The null space of $\mathcal{N}^+ + \mathcal{N}^-$ is trivial, and $\mathcal{N}^+ + \mathcal{N}^-$ is invertible.

Now we multiply (66) by the bounded $(\mathcal{N}_{00}^{(l)} + \mathcal{N}_{11}^{(l)})^{-1}$. Then the third term in the multiplied (66) is exponentially smaller than the second term, and the first term must be comparable to the second term. Thus, we approximate

$$(\mathcal{R}_p^+)^{2^l} \approx [\mathcal{N}_{11}^{(l)} + \mathcal{N}_{00}^{(l)}]^{-1}\mathcal{N}_{10}^{(l)}, \tag{73}$$

with a truncation error $\mathcal{O}(||(\mathcal{R}_p^+)^{2^l}||\,||(\mathcal{R}_p^-)^{2^l}||)$. Furthermore, we get $\mathcal{R}_p^+$ iteratively from

$$(\mathcal{R}_p^+)^{2^j} \approx [\mathcal{N}_{11}^{(j)} + \mathcal{N}_{00}^{(j)}]^{-1}\left[\mathcal{N}_{10}^{(j)} + \mathcal{N}_{01}^{(j)}(\mathcal{R}_p^+)^{2^{j+1}}\right], \quad j = l-1, \ldots, 0. \tag{74}$$

It can be seen clearly that the total truncation error for computing $\mathcal{R}_p^+$ accumulates to

$$\begin{aligned}
&\Pi_{j=l-1}^0 \left\{[\mathcal{N}_{11}^{(j)} + \mathcal{N}_{00}^{(j)}]^{-1}\mathcal{N}_{01}^{(j)}\right\} \mathcal{O}(\|(\mathcal{R}_p^+)^{2^l}\|\,\|(\mathcal{R}_p^-)^{2^l}\|)\\
&\quad = \mathcal{O}\left(\Pi_{j=l-1}^0 \left\{C\|[\mathcal{N}^+ + \mathcal{N}^-]^{-1}\|\|(\mathcal{R}_p^-)^{2^j}\|\right\} \|(\mathcal{R}_p^+)^{2^l}\|\,\|(\mathcal{R}_p^-)^{2^l}\|\right)\\
&\quad = \mathcal{O}\left(\left[C\|[\mathcal{N}^+ + \mathcal{N}^-]^{-1}\|\right]^l q^{0+1+\cdots+2^{l-1}} \|(\mathcal{R}_p^+)^{2^l}\|\,\|(\mathcal{R}_p^-)^{2^l}\|\right)\\
&\quad = \mathcal{O}\left(\|(\mathcal{R}_p^+)^{2^l}\|\,\|(\mathcal{R}_p^-)^{2^l}\|\right).
\end{aligned}$$

Consequently, the backward iteration (74) provides an exponentially accurate approximation to R_p^+ as $l \to \infty$. One similarly obtains $\mathcal{R}_p^-$ from

$$(\mathcal{R}_p^-)^{2^l} \approx [\mathcal{N}_{11}^{(l)} + \mathcal{N}_{00}^{(l)}]^{-1}\mathcal{N}_{01}^{(l)}, \tag{75}$$

$$(\mathcal{R}_p^-)^{2^j} \approx [\mathcal{N}_{11}^{(j)} + \mathcal{N}_{00}^{(j)}]^{-1}\left[\mathcal{N}_{01}^{(j)} + \mathcal{N}_{10}^{(j)}(\mathcal{R}_p^-)^{2^{j+1}}\right], \quad j = l-1, \ldots, 0. \tag{76}$$

According to Theorem 5.2, l can be chosen by the criteria

$$\max\{||\mathcal{N}_{00}^{(l)} - \mathcal{N}_{00}^{(l-1)}||, ||\mathcal{N}_{11}^{(l)} - \mathcal{N}_{11}^{(l-1)}||\} \le \epsilon_{\rm thres}$$

for some sufficiently small threshold parameter $\epsilon_{\rm thres} > 0$. Since this simple approach has been successful, we did not try alternative adaptive algorithms based, e.g., on a posteriori error estimates of the form $C\|\mathcal{N}_{l-1}^\pm - \mathcal{N}_l^\pm\|\,\|\tilde{u}^{og}\|$. Clearly, RDP does not

require solving any Sylvester equation and thus is more effective than the modified Newton's method in [22]. As shall be illustrated in numerical examples, RDP can provide sufficiently accurate numerical solutions by only a few iterations.

From the above, it can be seen that the essential step to approximating $\mathcal{N}^{\pm}$ is to get the NtD operator $\mathcal{N}^{(0)}$ on the boundary of the unit cell $\Omega_1^{\pm}$. As no information of the field $\tilde{u}^{\mathrm{og}}$ in $\Omega_1^{\pm}$ is required, it is clear that the BIE method is an optimal choice, as it treats only the boundary of $\Omega_1^{\pm}$. Since PML is involved in domain $\Omega_1^{\pm}$, the high-accuracy PML-based BIE method developed in our previous work [29] straightforwardly provides an accurate approximation of $\mathcal{N}^{(0)}$, so as to effectively drive the RDP to get $\mathcal{N}^{\pm}$ by (72). We shall present the details in the next section.

6. The PML-based BIE method. In this section, we shall first review the PML-based BIE method in [29] to approximate the NtD operator on the boundary of a unit cell—one with perturbation and one without—by an NtD matrix. Then, we shall use these NtD matrices to approximate the two vNtD operators $\mathcal{N}^{\pm}$ on $\Gamma_0^{\pm}$ and to solve (BVP1) finally. From now on, we shall assume that the scattering surface Γ is piecewise smooth and satisfies (GC).

6.1. Approximating $\mathcal{N}^{\pm}$. Without loss of generality, we consider (BVP2) in an unperturbed cell, say Ω_1^+, and we need to approximate $\mathcal{N}^{(0)}$ first. According to [29], for any $\tilde{u}$ satisfying

$$\nabla \cdot (\mathbf{A}\nabla\tilde{u}) + k^2\alpha\tilde{u} = 0 \tag{77}$$

on Ω_1^+, we have the Green representation theorem

$$\tilde{u}(x) = \int_{\partial\Omega_1^+} \{\tilde{G}(x,y)\partial_{\nu_c}\tilde{u}(y) - \partial_{\nu_c}\tilde{G}(x,y)\tilde{u}(y)\}ds(y) \tag{78}$$

for all $x \in \Omega_1^+$. We recall that ν denotes the outer unit normal vector on $\partial\Omega_1^+$ and $\nu_c := A\nu$ the conormal vector. Moreover, as x approaches $\partial\Omega_1^+ = \cup_{j=1}^4 \overline{\Gamma_{j,1}}$, the usual jump conditions imply [29]

$$\mathcal{K}[\tilde{u}](x) - \mathcal{K}_0[1](x)\tilde{u}(x) = \mathcal{S}[\partial_{\nu_c}\tilde{u}](x), \tag{79}$$

where we have defined the integral operators

$$\mathcal{S}[\phi](x) = 2\int_{\partial\Omega_1^+} \tilde{G}(x,y)\phi(y)ds(y), \tag{80}$$

$$\mathcal{K}[\phi](x) = 2\,\mathrm{p.v.}\int_{\partial\Omega_1^+} \partial_{\nu_c}\tilde{G}(x,y)\phi(y)ds(y), \tag{81}$$

$$\mathcal{K}_0[\phi](x) = 2\,\mathrm{p.v.}\int_{\partial\Omega_1^+} \partial_{\nu_c}\tilde{G}_0(x,y)\phi(y)ds(y), \tag{82}$$

where p.v. indicates the Cauchy principal value, and $\tilde{G}_0(x,y) = -\frac{1}{2\pi}\log\rho(\tilde{x},\tilde{y})$ is the fundamental solution of the complexified Laplace equation $\nabla(\mathbf{A}\cdot\nabla\tilde{u}) = 0$. Note that

$$\mathcal{K}_0[1](x) = -\frac{\theta^{\mathrm{in}}(x)}{\pi}, \tag{83}$$

where $\theta^{\mathrm{in}}(x)$ is defined as the interior angle at x, as indicated in Figure 4(b). However, numerically evaluating $\mathcal{K}_0[1]$ near corners is more advantageous, as illustrated in the

literature [13, 28]. Thus, $\tilde{u} = (\mathcal{K} - \mathcal{K}_0[1])^{-1}\mathcal{S}\partial_{\nu_c}\tilde{u}$ on $\partial\Omega_1^+$. Consequently, the NtD operator $\mathcal{N}_u$ for any unperturbed domain can be defined as

$$\mathcal{N}_u = (\mathcal{K} - \mathcal{K}_0[1])^{-1}\mathcal{S}.$$

Here and in the following, we denote the operator of multiplication with a function by the same symbol as that for the function. Note that some authors denote the operator of multiplication $\mathcal{K}_0[1]$ in the last formula by $\mathcal{K}_0[1]I$ and write $\mathcal{N}_u = (\mathcal{K} - \mathcal{K}_0[1]I)^{-1}\mathcal{S}$.

To approximate $\mathcal{N}_u$, we need to discretize the two integral operators and the multiplication operator on the right-hand side. Suppose now that the piecewise smooth curve $\partial\Omega_1^+$ is parameterized by $\{x(s) = (x_1(s), x_2(s))|\ 0 \le s \le L_1\}$, which is close to the arclength parameterization. Since corners may exist, $\tilde{u}(x(s))$ can have corner singularities in its derivatives at corners. To smoothen $\tilde{u}$, we introduce a grading function $s = w(t),\ 0 \le t \le 1$. For a smooth segment of $\partial\Omega_1^+$ corresponding to $s \in [s^0, s^1]$ and $t \in [t^0, t^1]$ such that $s^i = w(t^i)$ for $i = 0, 1$, where s^0 and s^1 correspond to two corners, we take [13, eq. (3.104)]

$$s = w(t) = \frac{s^0 w_1^p + s^1 w_2^p}{w_1^p + w_2^p}, \quad t \in [t^0, t^1], \tag{84}$$

where the positive integer p ensures that the derivatives of $w(t)$ vanish at the corners up to order p,

$$w_1 = \left(\frac{1}{2} - \frac{1}{p}\right)\xi^3 + \frac{\xi}{p} + \frac{1}{2}, \quad w_2 = 1 - w_1, \quad \xi = \frac{2t - (t^0 + t^1)}{t^1 - t^0}.$$

To simplify notation, we shall use $x(t)$ to denote $x(w(t))$, and $x'(t)$ to denote $\frac{dx}{ds}(w(t))w'(t)$, in the following. Assume that $[0, 1]$ is uniformly sampled by N grid points $\{t_j = jh\}_{j=1}^N$ with even N and grid size $h = 1/N$ and that the grid points contain all the corner points.

Thus, $\mathcal{S}[\partial_{\nu_c}\tilde{u}]$ at point $x = x(t_j)$ can be parameterized by

$$\mathcal{S}[\partial_{\nu_c}\tilde{u}](x(t_j)) = \int_0^1 S(t_j, t)\phi^{\mathrm{s}}(t)dt, \tag{85}$$

where $S(t_j, t) = \frac{\mathrm{i}}{2}H_0^{(1)}(k\rho(x(t_j), x(t)))$, and the scaled conormal vector $\phi^{\mathrm{s}}(t) = \partial_{\nu_c}\tilde{u}(x(t))|x'(t)|$, smoother than $\partial_{\nu_c}\tilde{u}(x(t))$, is introduced to regularize the approximation of $\mathcal{N}_u$ [27].

Considering the logarithmic singularity of $S(t_j, t)$ at $t = t_j$, we can discretize the integral in (85) by Alpert's 6th-order hybrid Gauss-trapezoidal quadrature rule [1] and then by trigonometric interpolation to get

$$\mathcal{S}[\partial_{\nu_c}\tilde{u}^s]\begin{bmatrix} x(t_1) \\ \vdots \\ x(t_N) \end{bmatrix} \approx \mathbf{S}\begin{bmatrix} \phi^{\mathrm{s}}(t_1) \\ \vdots \\ \phi^{\mathrm{s}}(t_N) \end{bmatrix}, \tag{86}$$

where the $N \times N$ matrix $\mathbf{S}$ approximates $\mathcal{S}$. One similarly approximates $\mathcal{K}[\tilde{u}](x(t_j))$ and $\mathcal{K}_0[1](x(t_j))$ for $j = 1, \ldots, N$, so that we obtain, on the boundary of $\partial\Omega_1^+$,

$$\begin{bmatrix} \boldsymbol{u}_{1,1} \\ \boldsymbol{u}_{1,2} \\ \boldsymbol{u}_{1,3} \\ \boldsymbol{u}_{1,4} \end{bmatrix} = \boldsymbol{N}_u \begin{bmatrix} \boldsymbol{\phi}^{\mathrm{s}}_{1,1} \\ \boldsymbol{\phi}^{\mathrm{s}}_{1,2} \\ \boldsymbol{\phi}^{\mathrm{s}}_{1,3} \\ \boldsymbol{\phi}^{\mathrm{s}}_{1,4} \end{bmatrix}, \tag{87}$$

where $\boldsymbol{u}_{1,j'}$ and $\boldsymbol{\phi}^s_{1,j'}$ for $j' = 1,2,3,4$ represent $N_{j'} \times 1$ column vectors of $\tilde{u}$ and $\phi^{\rm s}$ at the $N_{j'}$ grid points of $\Gamma_{1,j'}$, respectively. Note that $N = \sum_{j'=1}^{4} N_{j'}$, and the grid points on $\Gamma_{1,3}$ are obtained by horizontally shifting the grid points on $\Gamma_{1,1}$ to $\Gamma_{1,3}$ so that $N_1 = N_3$. Clearly, the $N \times N$ matrix $\boldsymbol{N}_u$ approximates the scaled NtD operator $\mathcal{N}_u^{\rm s}$ related to $\mathcal{N}_u$ by $\mathcal{N}_u \partial_{\nu_c} \tilde{u} = \mathcal{N}_u^{\rm s} \phi^{\rm s}$. Now, by $\tilde{u}|_{\Gamma_{1,2}\cup\Gamma_{1,4}} = 0$, we eliminate the vectors $\boldsymbol{u}_{1,2}$, $\boldsymbol{u}_{1,4}$, $\boldsymbol{\phi}_{1,2}$, and $\boldsymbol{\phi}_{1,4}$ in (87) so that we obtain two $2N_1 \times 2N_1$ matrices $\boldsymbol{N}^{(0)}$ and $\boldsymbol{T}$ that satisfy

$$\text{(88)} \qquad \begin{bmatrix} \boldsymbol{u}_{1,1} \\ \boldsymbol{u}_{1,3} \end{bmatrix} = \boldsymbol{N}^{(0)} \begin{bmatrix} \boldsymbol{\phi}^{\rm s}_{1,1} \\ \boldsymbol{\phi}^{\rm s}_{1,3} \end{bmatrix}, \quad \begin{bmatrix} \boldsymbol{\phi}^{\rm s}_{1,2} \\ \boldsymbol{\phi}^{\rm s}_{1,4} \end{bmatrix} = \boldsymbol{T} \begin{bmatrix} \boldsymbol{\phi}^{\rm s}_{1,1} \\ \boldsymbol{\phi}^{\rm s}_{1,3} \end{bmatrix},$$

where we denote

$$\boldsymbol{N}^{(0)} = \begin{bmatrix} \boldsymbol{N}^{(0)}_{00} & \boldsymbol{N}^{(0)}_{01} \\ \boldsymbol{N}^{(0)}_{10} & \boldsymbol{N}^{(0)}_{11} \end{bmatrix}$$

by $\boldsymbol{N}^{(0)}_{ij} \in \mathbb{C}^{N_1 \times N_1}$. On the continuous level, a representation like (88) follows from the well-posedness of (BVP2) in Theorem 5.1. So we presume that the elimination leading to (88) on the discretized level is stable. Note that, different from [29], we no longer simultaneously assume $\tilde{u} = \phi^{\rm s} = 0$ on the PML boundary $\Gamma_{1,4}$, which could cause pronounced errors in numerical results. A possible reason is as follows. Unlike [29], BIEs are used in all unit cells, no matter how close to or far away from the perturbed cell. For the cells away from the perturbed cell, a part of $\tilde{u}^{\rm og}$ can enter the PML at small grazing angles, so that inconsistently assuming both zero Dirichlet and Neumann conditions on $\Gamma_{1,4}$ leads to significant truncation errors. Now compare (56) and (88). Like $\boldsymbol{N}_u$, $\boldsymbol{N}^{(0)}$ approximates the scaled NtD operator $\mathcal{N}^{(0),{\rm s}}$ on $\Gamma_1^+ \cup \Gamma_3^+$ related to $\mathcal{N}^{(0)}$ by $\mathcal{N}^{(0)} \partial_{\nu_c} \tilde{u} = \mathcal{N}^{(0),{\rm s}} \phi^s$.

The PML-based BIE method can provide a high-accuracy approximation of $\mathcal{N}^{(0),s}$ based on two aspects. First, the grading function $w(t)$ smoothens the densities (e.g., $\phi^s(t)$ in (85)) in the integral operators $\mathcal{S}$, $\mathcal{K}$, and $\mathcal{K}_0$, as illustrated by [13, 29]. Second, the quadrature rule [1] is proved to be highly accurate for discretizing the three integral operators with logarithmic kernels (e.g., $S(t_j, t)$ in (85)) and smooth densities. Some numerical techniques, further stabilizing the numerical discretizations, have been presented in detail in [29].

Consequently, the previously developed RDP can be easily adapted here, in terms of notation, by replacing $\mathcal{N}$ by $\boldsymbol{N}$ for the equations (64)–(76), so that we get two $N_1 \times N_1$ matrices $\boldsymbol{R}_p^+$ and $\boldsymbol{N}^+$ approximating the (scaled) Neumann-marching operator $\mathcal{R}_p^+$ and the (scaled) vNtD operator $\mathcal{N}^+$ such that $\boldsymbol{\phi}^{\rm s}_{1,3} = -\boldsymbol{R}_p^+ \boldsymbol{\phi}^{\rm s}_{1,1}$ and $\boldsymbol{u}_{1,1} = \boldsymbol{N}^+ \boldsymbol{\phi}^{\rm s}_{1,1}$. One similarly obtains two $N_1 \times N_1$ matrices $\boldsymbol{R}_p^-$ and $\boldsymbol{N}^-$ approximating $\mathcal{R}_p^-$ and $\mathcal{N}^-$, respectively.

6.2. Solving (BVP1). We are now ready to use the PML-based BIE method to solve the main problem (BVP1). Fix $x^* \in \Omega_0$. To eliminate the δ function, we consider $\tilde{u}^{\rm sc}(x; x^*) = \tilde{u}^{\rm og}(x; x^*) - \tilde{u}^{\rm inc}(x; x^*)$, satisfying (77). For simplicity, we denote (cf. Figure 3(a))

$$\Gamma_{0,1} = \Gamma_0^-, \quad \Gamma_{0,2} = \Gamma_0, \quad \Gamma_{0,3} = \Gamma_0^+, \quad \text{and} \quad \Gamma_{0,4} = \Gamma_0^{H+L}.$$

Then, analogous to (87), on the four boundaries $\Gamma_{0,j}$, $j = 1,2,3,4$, we apply the PML-based BIE method of the previous section to approximate the NtD operator for

$\tilde{u}^{\rm sc}$ and $\partial_{\nu_c}\tilde{u}^{\rm sc}$ on the boundary of the perturbed cell Ω_0 by a matrix $\boldsymbol{N}_p$,

$$\begin{bmatrix} \boldsymbol{u}^{\rm sc}_{0,1} \\ \boldsymbol{u}^{\rm sc}_{0,2} \\ \boldsymbol{u}^{\rm sc}_{0,3} \\ \boldsymbol{u}^{\rm sc}_{0,4} \end{bmatrix} = \boldsymbol{N}_p \begin{bmatrix} \boldsymbol{\phi}^{\rm sc,s}_{0,1} \\ \boldsymbol{\phi}^{\rm sc,s}_{0,2} \\ \boldsymbol{\phi}^{\rm sc,s}_{0,3} \\ \boldsymbol{\phi}^{\rm sc,s}_{0,4} \end{bmatrix}, \tag{89}$$

where $\boldsymbol{u}^{\rm sc}_{0,j}$ and $\boldsymbol{\phi}^{\rm sc,s}_{0,j}$ for $j = 1, 2, 3, 4$ represent column vectors of $\tilde{u}^{\rm sc}$ and $\partial_{\nu_c}\tilde{u}^{\rm sc}|x'|$ at the grid points of $\Gamma_{0,j}$, respectively. Rewriting the above in terms of $\tilde{u}^{\rm og}$ and $\partial_{\nu_c}\tilde{u}^{\rm og}$, we get

$$\begin{bmatrix} \boldsymbol{u}^{\rm og}_{0,1} \\ \boldsymbol{u}^{\rm og}_{0,2} \\ \boldsymbol{u}^{\rm og}_{0,3} \\ \boldsymbol{u}^{\rm og}_{0,4} \end{bmatrix} = \boldsymbol{N}_p \begin{bmatrix} \boldsymbol{\phi}^{\rm og,s}_{0,1} \\ \boldsymbol{\phi}^{\rm og,s}_{0,2} \\ \boldsymbol{\phi}^{\rm og,s}_{0,3} \\ \boldsymbol{\phi}^{\rm og,s}_{0,4} \end{bmatrix} + \begin{bmatrix} \boldsymbol{u}^{\rm inc}_{0,1} \\ \boldsymbol{u}^{\rm inc}_{0,2} \\ \boldsymbol{u}^{\rm inc}_{0,3} \\ \boldsymbol{u}^{\rm inc}_{0,4} \end{bmatrix} - \boldsymbol{N}_p \begin{bmatrix} \boldsymbol{\phi}^{\rm inc,s}_{0,1} \\ \boldsymbol{\phi}^{\rm inc,s}_{0,2} \\ \boldsymbol{\phi}^{\rm inc,s}_{0,3} \\ \boldsymbol{\phi}^{\rm inc,s}_{0,4} \end{bmatrix}, \tag{90}$$

where $\boldsymbol{u}^{\rm inc}_{0,j}$ and $\boldsymbol{\phi}^{\rm inc,s}_{0,j}$ represent column vectors of $\tilde{u}^{\rm inc}(x; x^*)$ and $\partial_{\nu_c}\tilde{u}^{\rm inc}(x; x^*)|x'|$ at the grid points of $\Gamma_{0,j}$, respectively. The boundary conditions in (BVP1) imply that

$$\boldsymbol{u}^{\rm og}_{0,2} = 0, \quad \boldsymbol{u}^{\rm og}_{0,4} = 0, \tag{91}$$

$$\boldsymbol{u}^{\rm og}_{0,1} = \boldsymbol{N}^{-}\boldsymbol{\phi}^{\rm og,s}_{0,1}, \quad \boldsymbol{u}^{\rm og}_{0,3} = \boldsymbol{N}^{+}\boldsymbol{\phi}^{\rm og,s}_{0,3}. \tag{92}$$

Solving the linear system (90)–(92), we get $\tilde{u}^{\rm og}(x; x^*)$ and $\partial_{\nu_c}\tilde{u}^{\rm og}(x; x^*)$ on all grid points of $\partial\Omega_0$.

Now we discuss how to evaluate $\tilde{u}^{\rm og}(x; x^*)$ in the physical domain S_H. We distinguish two cases:

1. $x \in \Omega_0$. Since on the grid points of $\partial\Omega_0$, $\tilde{u}^{\rm sc}$ and $\partial_{\nu_c}\tilde{u}^{\rm sc}|x'|$ are available, we use the Green representation formula (78) with $\partial\Omega_1^+$ replaced by $\partial\Omega_0$ to compute $\tilde{u}^{\rm sc}(x; x^*)$ in Ω_0 so that $\tilde{u}^{\rm og}(x; x^*)$ becomes available in Ω_0.
2. $x \in \Omega_j^{\pm}$. Consider Ω_1^+ first. Suppose $\boldsymbol{u}^{\rm og}_{1,j'}$ and $\boldsymbol{\phi}^{\rm og,s}_{1,j'}$ represent column vectors of $\tilde{u}^{\rm og}$ and $\partial_{\nu_c}\tilde{u}^{\rm og}|x'|$ at the grid points of $\Gamma_{1,j'}$ for $1 \le j' \le 4$. By the continuity of $\partial_{\nu_c}\tilde{u}^{\rm og}$ on $\Gamma_{1,1} = \Gamma_{0,3} = \Gamma_0^+$, $\boldsymbol{\phi}^{\rm og,s}_{1,1} = -\boldsymbol{\phi}^{\rm og,s}_{0,3}$. Since $\boldsymbol{\phi}^{\rm og,s}_{1,3} = -\boldsymbol{R}_p^+\boldsymbol{\phi}^{\rm og,s}_{1,1}$, we get $\boldsymbol{u}^{\rm og}_{1,j'}$ for $j' = 1, 3$ by (88), and $\boldsymbol{\phi}^{\rm og,s}_{1,j'}$ for $j' = 2, 4$. Using $\boldsymbol{u}^{\rm og}_{1,2} = \boldsymbol{u}^{\rm og}_{1,4} = 0$, the functions $\tilde{u}^{\rm og}(x; x^*)$ and $\partial_{\nu_c}\tilde{u}^{\rm og}|x'|$ on $\partial\Omega_1^+$ become available. Hence, the Green representation formula (78) applies and provides $\tilde{u}^{\rm og}(x; x^*)$ in Ω_1^+. Repeating the same procedure, one obtains $\tilde{u}^{\rm og}(x; x^*)$ in Ω_j^+ for $j \ge 2$. The case for $x \in \Omega_j^-$ can be handled similarly.

Consequently, $u^{\rm tot}(x; x^*) \approx \tilde{u}^{\rm og}(x; x^*)$ becomes available for

$$x \in S_H \subset \overline{\Omega}_0 \cup \left[\cup_{j=1}^{\infty}\overline{\Omega}_{j,+} \cup \overline{\Omega}_{j,-}\right].$$

6.3. Computing $u^{\rm tot}$ for plane-wave incidence. To close this section, we briefly discuss how to compute $u^{\rm tot}$ for an incident plane wave $u^{\rm inc} = e^{\mathbf{i}k(\cos\theta x_1 - \sin\theta x_2)}$ with $\theta \in (0, \pi)$. First, we consider the unperturbed case $\Gamma = \Gamma_T$ so that $u^{\rm tot}$ becomes the reference solution $u^{\rm tot}_{\rm ref}$. It is clear that $u^{\rm sc}_{\rm ref} = u^{\rm tot}_{\rm ref} - u^{\rm inc}$ satisfies the quasi-periodic boundary condition

$$u^{\rm sc}_{\rm ref}(-T/2, x_2) = \gamma u^{\rm sc}_{\rm ref}(T/2, x_2), \tag{93}$$

$$\partial_{x_1} u^{\rm sc}_{\rm ref}(-T/2, x_2) = \gamma \partial_{x_1} u^{\rm sc}_{\rm ref}(T/2, x_2), \tag{94}$$

where $\gamma = e^{\mathbf{i}k\cos\theta\, T}$. On Γ, (2) implies

$$u^{\rm sc}_{\rm ref} = -u^{\rm inc}. \tag{95}$$

Due to quasi-periodicity, we could express $u^{\rm sc}_{\rm ref}$ above Γ_H in terms of a Fourier series, i.e.,

$$u^{\rm sc}_{\rm ref}(x_1,x_2) = \sum_{j=-\infty}^{\infty} R_j e^{\mathbf{i}\alpha_j x_1 + \mathbf{i}\beta_j x_2}, \quad x_2 \geq H, \tag{96}$$

where $\alpha_j = k\cos\theta + \frac{2\pi j}{T}$ and $\beta_j = \sqrt{k^2-\alpha_j^2}$ if $|\alpha_j| \leq k$ (otherwise, $\beta_j = \mathbf{i}\sqrt{\alpha_j^2-k^2}$), and R_j denotes the jth Rayleigh coefficient of the reflected wave. Thus, on the PML boundary Γ_{L+H}, the complexified field $\tilde{u}^{\rm sc}_{\rm ref}(x_1,x_2) = u^{\rm sc}_{\rm ref}(x_1,\tilde{x}_2)$ satisfies

$$\tilde{u}^{\rm sc}_{\rm ref}(x_1,L+H) = \sum_{j=-\infty}^{\infty} R_j e^{\mathbf{i}\alpha_j x_1 + \mathbf{i}\beta_j(H+L) - \beta_j S_c L}. \tag{97}$$

For simplicity, we assume that all β_j are sufficiently away from 0 so that, provided S_cL is sufficiently large, we can directly impose the following Dirichlet boundary condition:

$$\tilde{u}^{\rm sc}_{\rm ref}(x_1,H+L) = 0. \tag{98}$$

If β_j is quite close to 0, alternative accurate boundary conditions can be developed. We refer the reader to [26, 30, 35] for details. On the other hand, $\tilde{u}^{\rm sc}_{\rm ref}$ satisfies the quasi-periodic conditions (93) and (94) and the boundary condition (95), but with u replaced by $\tilde{u}$.

On the boundary $\partial\Omega_0$, the PML-BIE method gives, analogous to (89),

$$\begin{bmatrix} \boldsymbol{u}_1^{\rm sc} \\ \boldsymbol{u}_2^{\rm sc} \\ \boldsymbol{u}_3^{\rm sc} \\ \boldsymbol{u}_4^{\rm sc} \end{bmatrix} = \boldsymbol{N}_p \begin{bmatrix} \boldsymbol{\phi}_1^{\rm sc} \\ \boldsymbol{\phi}_2^{\rm sc} \\ \boldsymbol{\phi}_3^{\rm sc} \\ \boldsymbol{\phi}_4^{\rm sc} \end{bmatrix}, \tag{99}$$

where $\boldsymbol{u}_{j'}^{\rm sc}$ and $\boldsymbol{\phi}_{j'}^{\rm sc}$ for $1 \leq j' \leq 4$ represent vectors of values of $\tilde{u}^{\rm sc}_{\rm ref}$ and $\partial_{\nu_c}\tilde{u}^{\rm sc}_{\rm ref}|w'|$ at the grid points of $\Gamma_{0,j'}$, respectively. Note that $\boldsymbol{N}_p$ is the same as $\boldsymbol{N}_u$ in (87) since $\Gamma = \Gamma_T$. Equation (98) directly implies that

$$\boldsymbol{u}_4^{\rm sc} = 0. \tag{100}$$

The quasi-periodic conditions (93) and (94) imply

$$\boldsymbol{u}_3^{\rm sc} = \gamma \boldsymbol{u}_1^{\rm sc}, \quad \boldsymbol{\phi}_3^{\rm sc} = -\gamma \boldsymbol{\phi}_1^{\rm sc}. \tag{101}$$

The boundary condition (95) indicates

$$\boldsymbol{u}_2^{\rm sc} = -\boldsymbol{u}_2^{\rm inc}, \tag{102}$$

where $\boldsymbol{u}_2^{\rm inc}$ represents the vector of values of $u^{\rm inc}$ at grid points of $\Gamma_{0,2}$. Solving the linear system (99)–(102) gives rise to values of $\tilde{u}^{\rm sc}_{\rm ref}$ and $\partial_{\nu_c}\tilde{u}^{\rm sc}_{\rm ref}|w'|$ on $\partial\Omega_0$. The Green representation formula (78) can help to compute $\tilde{u}^{\rm sc}_{\rm ref}$ in Ω_0. The quasi-periodicity helps to construct $\tilde{u}^{\rm sc}_{\rm ref}$ in any other cell $\Omega_j^{\pm}$ for $j \in \mathbb{N}^*$. Consequently, $u^{\rm tot}_{\rm ref}$ becomes available in the whole physical domain S_H.

Now, if Γ is a local perturbation of Γ_T, then $\tilde{u}^{\rm sc}_{\rm ref}$ is available by the above arguments, and one follows the same approach developed in section 6.2 to get $\tilde{u}^{\rm og} = \tilde{u}^{\rm sc} - \tilde{u}^{\rm sc}_{\rm ref}$ in any unperturbed cell and, therewith, $u^{\rm tot}$ in the complete physical region S_H. We omit the details here.

7. Numerical examples. In this section, we will carry out four numerical experiments to validate the performance of the PML-based BIE method and the proposed theory. In all examples, we set the period to $T = 1$ and the wavelength to the free-space value $\lambda = 1$ so that $k_0 = 2\pi$. We consider two types of incidence: (1) a cylindrical incidence excited by the source point $x^* = (0, 1.5)$; and (2) a plane-wave incidence of angle θ to be specified. We suppose that only one unit cell of the periodic background structure is perturbed. To set up the PML, we choose $m = 0$ in (17) to simplify the definition of σ. In the RDP iterations (74) and (76), we take $l = 20$ and $\epsilon_{\text{thres}} = 10^{-15}$. Furthermore, we choose $H = 3$ and set the computational domain to be $[-5.5, 5.5] \times [-2, 3]$, which contains 11 cells. To validate the accuracy of our method, we compute the relative error

$$E_{\text{rel}} := \frac{||(\boldsymbol{\phi}_{2,0}^{\text{sc,s}})^{\text{num}} - (\boldsymbol{\phi}_{2,0}^{\text{sc,s}})^{\text{exa}}||_\infty}{||(\boldsymbol{\phi}_{2,0}^{\text{sc,s}})^{\text{exa}}||_\infty},$$

for $\boldsymbol{\phi}_{2,0}^{\text{sc,s}}$ representing the scaled normal derivative $|w'|\partial_\nu u^{\text{sc}}$ on $\Gamma_{2,0}$, the perturbed part of Γ, and for different values of S and L in the setup of the PML, where superscript "num" indicates a numerical solution and superscript "exa" a sufficiently accurate numerical solution or, if available, the exact solution.

Example 1: A flat curve. In the first example, we assume that Γ is the straight line $\{x : x_2 = 0\}$. Certainly, we can regard such a simple structure as a periodic structure with period equal to one wavelength. Formally, we regard the line segment $\Gamma_{0,2} \subset \Gamma$ between $x_1 = -0.5$ and $x_1 = 0.5$ as the "perturbed" part. For the cylindrical incidence, the total wave field u^{tot} is given by

$$u^{\text{tot}}(x; x^*) = \frac{\mathbf{i}}{4}\left[H_0^{(1)}(k|x - x^*|) - H_0^{(1)}(k|x - x^*_{\text{imag}}|)\right],$$

where the image source point is $x^*_{\text{imag}} = (0, -1.5)$. Using this to compute the scaled conormal derivative on segment $\Gamma_{0,2}$, we get the reference solution and can check the accuracy of our method. We discretize each smooth segment of the "perturbed"/unperturbed unit cell by 600 grid points. To check how the wavenumber condition in Theorem 5.1 affects the accuracy of our numerical solver, we consider two values of the refractive index n in Ω: (1) $n = 1.03$ so that $kT/\pi = 2.06 \notin \mathcal{E}$, and (2) $n = 1$ so that $kT/\pi = 2 \in \mathcal{E}$. For both cases, we compare results of Dirichlet and Neumann boundary conditions on Γ_{H+L}.

For $n = 1.03$, Figures 5(a) and (b) compare the exact solution and our numerical solution for $L = 2.2$ and $S = 2.8$. The two solutions are indistinguishable. To give a detailed comparison, Figures 5(c) and (d) show how the relative error E_{rel} decays as one of the two PML parameters, the absorbing constant S and the thickness L, increases for either zero Dirichlet or zero Neumann condition on Γ_{H+L}. In Figure 5(c), we take $L = 2.2$ and let S vary between 0.2 and 2.8, while in Figure 5(d), we take $S = 2.8$ and let the PML thickness L vary between 0.2 and 2.2. In both figures, the vertical axis is logarithmically scaled so that the vertical dashed lines indicate that the relative error E_{rel} decays exponentially as L or S increases for both conditions. On the other hand, the Neumann condition gives faster convergence rates than the Dirichlet condition. The convergence curves indicate that nearly 11 significant digits are revealed by the proposed PML-based BIE method. The "o" lines in Figure 6(a) show the convergence curve of

$$E_{\text{Ric}} = ||\boldsymbol{N}_{10}^{(0)} - [\boldsymbol{N}_{11}^{(0)} + \boldsymbol{N}_{00}^{(0)}]\boldsymbol{R}_p^+ + \boldsymbol{N}_{01}^{(0)}(\boldsymbol{R}_p^+)^2||_\infty \tag{103}$$

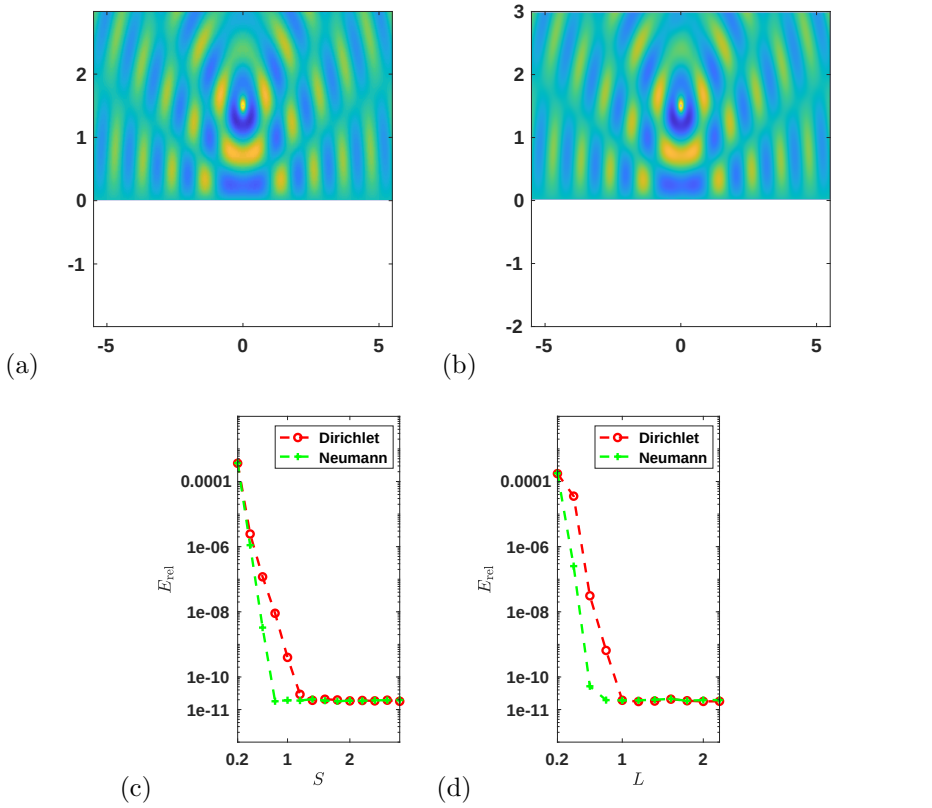

FIG. 5. *Example* 1: *Real part of* $u^{\rm tot}$ *in* $[-5.5,5.5]\times[-2.0,3.0]$ *excited by the point source* $y=(0,1.5)$. (a) *Exact solution.* (b) *Numerical solution. Convergence history of relative error* $E_{\rm rel}$ *versus* (c) *PML absorbing constant* S. (d) *Thickness of the PML* L *for both Dirichlet and Neumann conditions on* Γ_{H+L}.

against the number of iterations l. It can be seen that, after no more than 11 iterations, $\boldsymbol{R}_p^+$ converges exponentially and satisfies its governing Riccati equation (58) up to round-off errors. The "o" lines in Figure 6(b) show the curve of $||\phi^{\rm og,s}|_{\Gamma_j^+}||_\infty$ against j, where $\phi^{\rm og,s}$ denotes the scaled conormal derivative $|w'|\partial_{\nu_c^+}u^{\rm og}$. It can be seen that $\phi^{\rm og,s}$, and hence $\partial_{\nu_c^+}u^{\rm og}$, indeed decays exponentially as j or x_1 increases, as has been claimed in Corollary 5.1.

In Figure 6(c), we compare the Dirichlet and Neumann conditions for $n=1$. We take $L=2.2$ and let S vary from 0.2 to 2.8. Among the four convergence curves, solid lines indicate 600 grid points chosen on each smooth segment of each unit cell, while dashed lines indicate 100 grid points; "+" indicates the Neumann condition on Γ_{H+L} while "o" indicates the Dirichlet condition. If 100 grid points are used, $E_{\rm rel}$ for Neumann condition starts decreasing after $S\geq 2$, whereas $E_{\rm rel}$ for the Dirichlet condition has already reached its minimum error; if 600 grid points are used, the Neumann condition does not lead to a convergent $E_{\rm rel}$ at all for $S\in[0.2,2.8]$, but the Dirichlet condition still shows the same convergence rate and accuracy as in the case $n=1.03$. Consequently, the Dirichlet condition outperforms the Neumann condition for $n=1$.

Example 2: A sine curve. In the second example, we assume that Γ is the

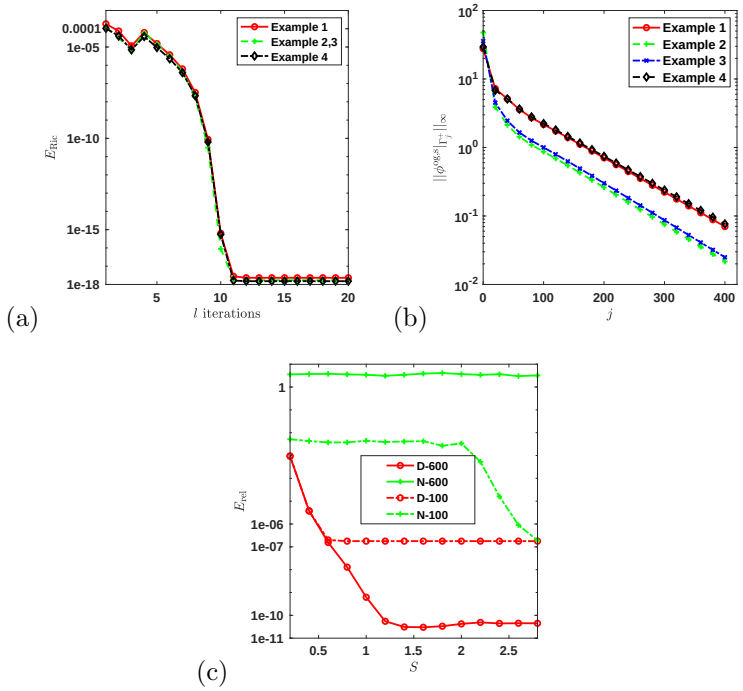

FIG. 6. *All four examples.* (a) *Convergence history of* $E_{\rm Ric}$ *in* (103) *against the number of iterations* l. (b) *Radiation behavior of* $\phi^{\rm og,s}|_{\Gamma_j^+}$ *as* $j \to \infty$. (c) *Performance of Dirichlet and Neumann conditions in Example* 1 *for* $n = 1$, *at which* $kT/\pi \in \mathcal{E}$; *here "D" stands for Dirichlet and "N" for Neumann, and* 100 *indicates* 100 *grid points are used to discretize each smooth segment of the unit cells, etc.*

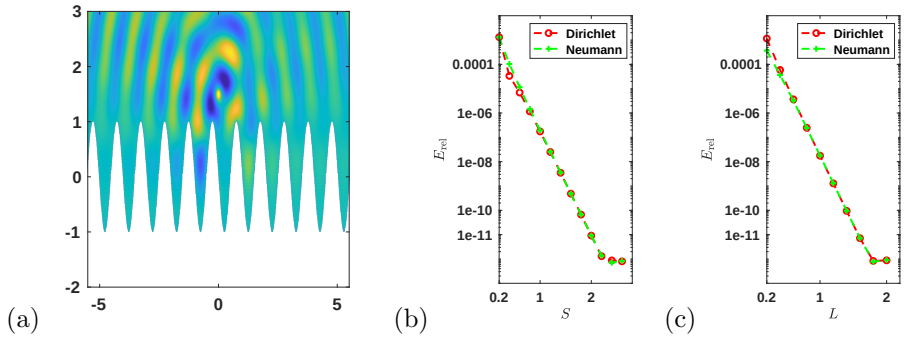

FIG. 7. *Example* 2. (a) *Numerical solution of real part of the total wave field* u *in* $[-5.5, 5.5]\times[-2.0, 3.0]$ *excited by the point source* $y=(0, 1.5)$. *Convergence history of relative error* $E_{\rm rel}$ *versus* (b) *PML absorbing constant* S *for fixed PML thickness* $L=2$, *and* (c) *PML thickness* L *for fixed PML absorbing constant* $S=2.8$; *vertical axes are logarithmically scaled.*

sine curve, $x_2 = \sin(2\pi x_1 + \pi)$, as shown in Figure 7(a) and that $n = 1.03$ to obtain $kT/\pi \notin \mathcal{E}$. For the cylindrical incidence, we discretize each smooth segment of any unit cell by 600 grid points and compare results of the Dirichlet and Neumann boundary conditions on Γ_{H+L}. Taking $S = 2.8$ and $L = 2.2$, we evaluate the wave field in $[-5.5, 5.5]\times[-2.0, 3.0]$ and use this as the reference solution since the exact solution is

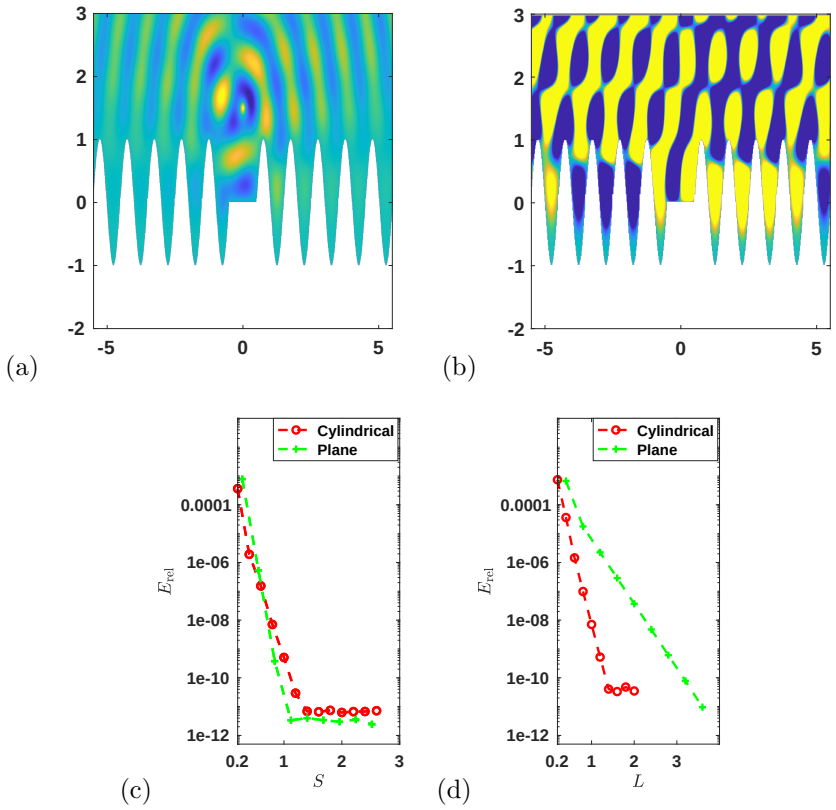

FIG. 8. *Example* 3. *Numerical solution of real part of the total wave field* u *in* $[-5.5, 5.5] \times [-2.0, 3.0]$ *excited by* (a) *a cylindrical wave by source* $y = (0, 1.5)$*;* (b) *a plane wave of incident angle* $\theta = \frac{\pi}{3}$*. Convergence history of relative error* $E_{\rm rel}$ *versus* (c) *PML thickness* L *for fixed PML absorbing constant* $S = 2.8$ *for both incidences, and* (d) *PML absorbing constant* S *for fixed PML thickness* $L = 2.2$ *(4.0) for cylindrical (plane-wave) incidence.*

no longer available. In Figure 7, (a) shows the field pattern of the reference solution, and (b) and (c) show the convergence history of relative error $E_{\rm rel}$ versus one of the two PML parameters S and L, respectively. Again, we observe that $E_{\rm rel}$ decays exponentially as S or L increases, and that nearly 12 significant digits are revealed by the proposed PML-based BIE method. Unlike the flat surface in Example 1, we no longer observe a faster convergence rate of the Neumann condition, but find that both conditions share the same convergence rate and accuracy. Comparing with the bad result for the Dirichlet condition and $kT/\pi \in \mathcal{E}$ and with the impressive improvement for $kT/\pi \notin \mathcal{E}$, we conclude that, in the sine curve example, the Neumann condition is less superior than the Dirichlet condition, and thus we shall only use the latter in the remaining experiments. With the Dirichlet condition, the "+" lines in Figure 6(a) show the convergence curve of $E_{\rm Ric}$ in (103) against the number of iterations l. The "+" lines in Figure 6(b) show the curve of $||\phi^{\rm og,s}|_{\Gamma_j^+}||_\infty$ against j.

Example 3: A locally perturbed sine curve. In the third example, we assume that Γ is the sine curve $\Gamma_T := \{x : x_2 = \sin(2\pi x_1 + \pi)\}$ locally perturbed such that the part between $x_1 = -0.5$ and $x_1 = 0.5$ is replaced by the line segment $\{(x_1, 0) : x_1 \in [-0.5, 0.5]\}$, as shown in Figure 8(a). For the cylindrical incidence, we

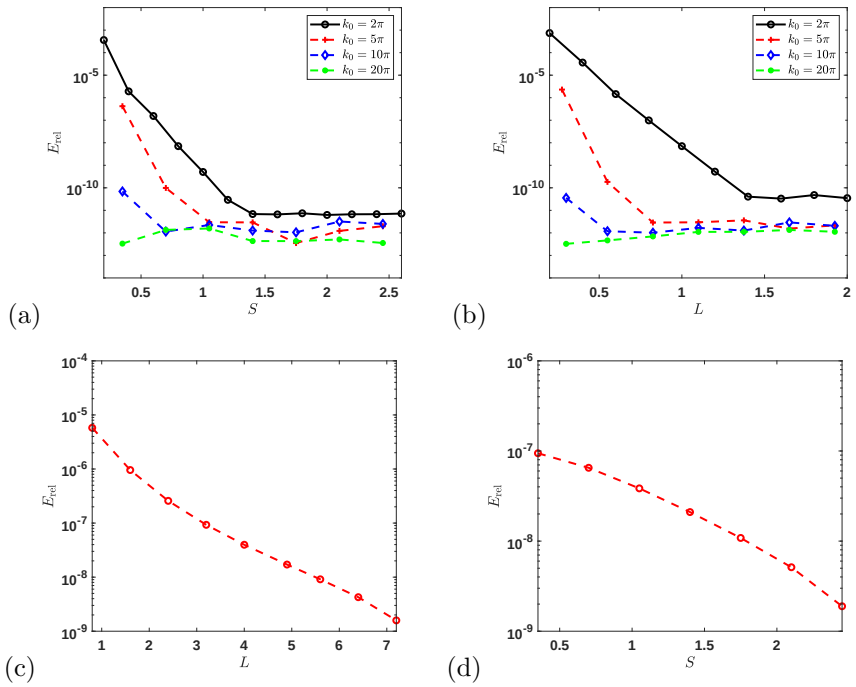

FIG. 9. *Example* 3. *For* $n = 1.03$, *the cylindrical incidence, and different values of* k_0, *convergence history of relative error* $E_{\rm rel}$ *versus* (a) *PML thickness* L *for fixed PML absorbing constant* $S = 2.8$, (b) *PML absorbing constant* S *for fixed PML thickness* $L = 2.2$. *For* $n = 1$, *the cylindrical incidence, and* $k_0 = 2\pi$, *convergence history of relative error* $E_{\rm rel}$ *versus* (c) *PML thickness* L *for fixed PML absorbing constant* $S = 2.8$, *and* (d) *PML absorbing constant* S *for fixed PML thickness* $L = 8$.

discretize each smooth segment of any unit cell by 600 grid points. Taking $S = 2.8$ and $L = 2.2$, we evaluate the wave field in $[-5.5, 5.5] \times [-2.0, 3.0]$ and use this as the reference solution, the field pattern of which is shown in Figure 8(a). The "x" lines in Figure 6(b) show the curve of $||\phi^{\rm og,s}|_{\Gamma_j^+}||_\infty$ against j.

For the plane-wave incidence, we take $\theta = \frac{\pi}{3}$ and discretize each smooth segment of any unit cell by 700 grid points. Taking $S = 2.8$ and $L = 4$, we evaluate the wave field in $[-5.5, 5.5] \times [-2.0, 3.0]$ and use this as the reference solution, the field pattern of which is shown in Figure 8(b).

For both incidences, Figures 8(c) and (d) show the convergence history of relative error $E_{\rm rel}$ versus one of the two PML parameters S and L, respectively. The convergence curves decay exponentially and indicate that nearly 11 significant digits are revealed by the proposed PML-based BIE method.

For the cylindrical incidence, in Figures 9(a) and (b) we show the convergence history of relative error $E_{\rm rel}$ versus the PML parameters S and L, with k_0 being one of the four values $2\pi, 5\pi, 10\pi$, and 20π, where numerical solutions for $S = 2.8$ and $L = 2.2$ are used as the reference solutions. It can be seen that $E_{\rm rel}$ reaches the round-off error more rapidly as k_0 increases. In other words, to attain a specified accuracy, S and L can be made smaller for an incident wave with a greater wavenumber (or a smaller wavelength), which is a common fact for the PML community [21]. For $k_0 = 2\pi$ and $n = 1$ so that $kT/\pi \in \mathcal{E}$, in Figures 9(c) and (d) we show the convergence

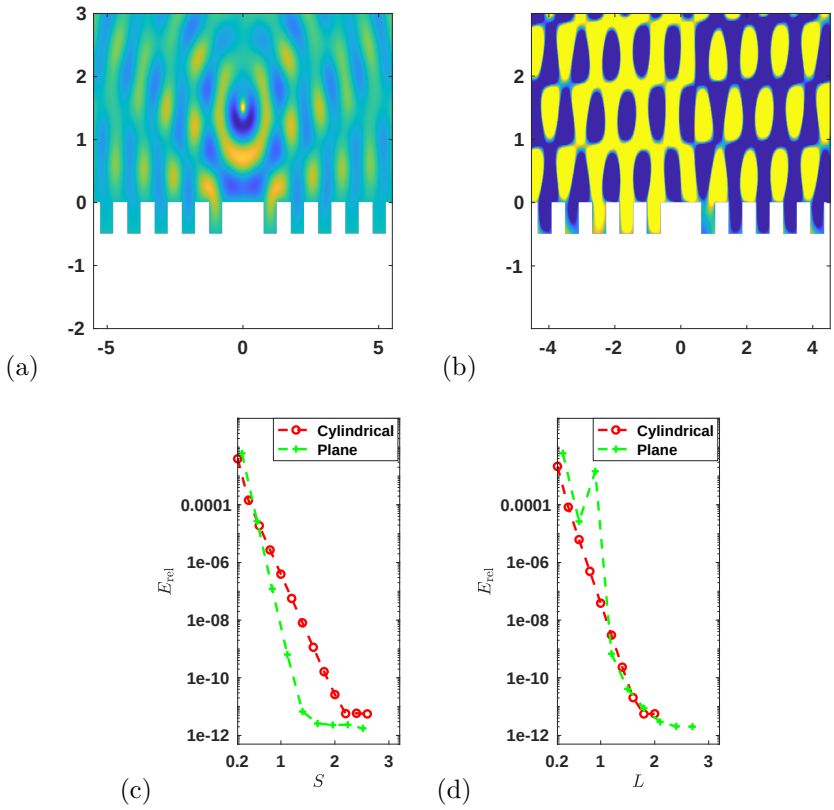

FIG. 10. *Example* 4. *Numerical solution of real part of the total wave field* u *in* $[-5.5,5.5]\times[-2.0,3.0]$ *excited by* (a) *a cylindrical wave by source* $y=(0,1.5)$, (b) *a plane wave of incident angle* $\theta=\frac{\pi}{6}$. *Convergence history of relative error* $E_{\rm rel}$ *versus* (c) *PML thickness* L *for fixed PML absorbing constant* $S=2.8$ *for both incidences, and* (d) *PML absorbing constant* S *for fixed PML thickness* $L=2.2$ *(*3.0*) for cylindrical (plane-wave) incidence.*

curves for $E_{\rm rel}$ against S or L, where a numerical solution for $S=2.8$ and $L=8$ is used as the reference solution. Unlike in previous results, here L is chosen to be 8 wavelengths long to obtain 9 significant digits. Such a thicker PML is required since $\tilde{u}^{\rm og}$ decays more slowly in the PML region, which is possibly caused by the existence of eigenfunctions in the semiwaveguides. Nevertheless, it can be seen that $E_{\rm rel}$ still decays exponentially as the PML parameters S and L increase.

Example 4: A locally perturbed binary grating. In the last example, we assume that Γ consists of periodic rectangular grooves of depth 0.5 and width 0.25, with the part between $x_1=-0.5$ and $x_1=0.5$ replaced by the line segment $\{(x_1,0)\colon x_1\in[-0.5,0.5]\}$, as shown in Figure 10(a). For the cylindrical incidence, we discretize each smooth segment of any unit cell by 600 grid points. Taking $S=2.8$ and $L=2.2$, we evaluate the wave field in $[-5.5,5.5]\times[-2.0,3.0]$ and use this as the reference solution, the field pattern of which is shown in Figure 10(a). The "$\Diamond$" lines in Figure 6(a) show the convergence curve of $E_{\rm Ric}$ in (103) against the number of iterations l. The "$\Diamond$" lines in Figure 6(b) show the curve of $||\phi^{\rm og,s}|_{\Gamma_j^+}||_\infty$ against j.

For the plane-wave incidence, we take $\theta=\frac{\pi}{6}$ and discretize each smooth segment of any unit cell by 600 grid points. Taking $S=2.8$ and $L=3$, we evaluate the wave

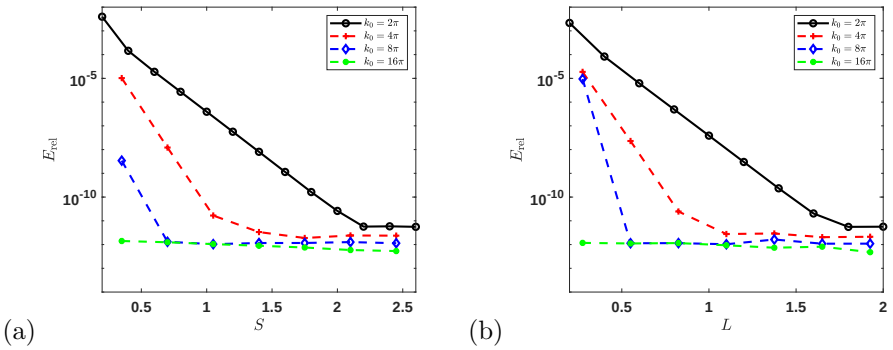

FIG. 11. *Example* 4. *For cylindrical incidence and for different values of* k_0*, convergence history of relative error* $E_{\rm rel}$ *versus* (a) *PML thickness* L *for fixed PML absorbing constant* $S=2.8$, (b) *PML absorbing constant* S *for fixed PML thickness* $L=2.2$.

field in $[-5.5, 5.5]\times[-2.0, 3.0]$ and use this as the reference solution, the field pattern of which is shown in Figure 10(b).

For both incidences, Figures 10(c) and (d) show the convergence history of relative error $E_{\rm rel}$ versus one of the two PML parameters S and L, respectively. The convergence curves decay exponentially and indicate that nearly 12 significant digits are revealed by the proposed PML-based BIE method. For the cylindrical incidence, in Figures 11(a) and (b) we show the convergence history of relative error $E_{\rm rel}$ versus the PML parameters S and L, with k_0 being one of the four values $2\pi, 4\pi, 8\pi$, and 16π, where numerical solutions for $S = 2.8$ and $L = 2.2$ are used as the reference solutions.

8. Conclusion. This paper studied the perfectly matched layer (PML) theory for wave scattering in a half space of a homogeneous medium bounded by a two-dimensional, perfectly conducting, and locally defected periodic surface, and developed a high-accuracy boundary integral equation (BIE) solver. By placing a PML in the vertical direction to truncate the unbounded domain to a strip, we proved that the PML solution converges to the true solution in the physical subregion of the strip at an algebraic order of the PML thickness. Laterally, the unbounded strip is divided into three regions: a region containing the defect, and two semi-waveguide regions of periodic subsurfaces, all separated by two vertical line segments. We proved the well-posedness of an associated scattering problem in both semi-waveguides so as to well define a Neumann-to-Dirichlet (NtD) operator on the associated vertical segment. The two NtD operators, serving as exact lateral boundary conditions, reformulate the unbounded strip problem as a boundary value problem over the defected region. Each NtD operator is closely related to a Neumann-marching operator, governed by a nonlinear Riccati equation, which was efficiently solved by an RDP method and a high-accuracy PML-based BIE method so that the boundary value problem on the defected region finally can be solved.

Our future research plan shall focus on the following two aspects:

(1) Extending the current work to study locally defected periodic structures of stratified media. In such case, propagating Bloch modes may exist so that the related Neumann marching operators $\mathcal{R}_p^{\pm}$ may not be contracting.

(2) Rigorously justifying that the PML solution converges exponentially to the true solution in any compact subset of the strip, as has been demonstrated by numerical experiments.

REFERENCES

[1] B. K. Alpert, *Hybrid Gauss-trapezoidal quadrature rules*, SIAM J. Sci. Comput., 20 (1999), pp. 1551–1584, https://doi.org/10.1137/S1064827597325141.

[2] T. Arens and T. Hohage, *On radiation conditions for rough surface scattering problems*, IMA J. Appl. Math., 70 (2005), pp. 839–847.

[3] G. Bao, D. C. Dobson, and J. A. Cox, *Mathematical studies in rigorous grating theory*, J. Opt. Soc. Amer. A, 12 (1995), pp. 1029–1042.

[4] J.-P. Berenger, *A perfectly matched layer for the absorption of electromagnetic waves*, J. Comput. Phys., 114 (1994), pp. 185–200.

[5] S. N. Chandler-Wilde and J. Elschner, *Variational approach in weighted Sobolev spaces to scattering by unbounded rough surfaces*, SIAM J. Math. Anal., 42 (2010), pp. 2554–2580, https://doi.org/10.1137/090776111.

[6] S. N. Chandler-Wilde and P. Monk, *The PML for rough surface scattering*, Appl. Numer. Math., 59 (2009), pp. 2131–2154.

[7] S. N. Chandler-Wilde and P. Monk, *Existence, uniqueness and variational methods for scattering by unbounded rough surfaces*, SIAM J. Math. Anal., 37 (2005), pp. 598–618, https://doi.org/10.1137/040615523.

[8] S. N. Chandler-Wilde, C. R. Ross, and B. Zhang, *Scattering by infinite one-dimensional rough surfaces*, R. Soc. Lond. Proc. Ser. A Math. Phys. Eng. Sci., 455 (1999), pp. 3767–3787.

[9] S. N. Chandler-Wilde and B. Zhang, *Electromagnetic scattering by an inhomogeneous conducting or dielectric layer on a perfectly conducting plate*, R. Soc. Lond. Proc. Ser. A Math. Phys. Eng. Sci., 454 (1998), pp. 519–542.

[10] Z. Chen and H. Wu, *An adaptive finite element method with perfectly matched absorbing layers for the wave scattering by periodic structures*, SIAM J. Numer. Anal., 41 (2003), pp. 799–826, https://doi.org/10.1137/S0036142902400901.

[11] W. C. Chew, *Waves and Fields in Inhomogeneous Media*, IEEE Press, New York, 1995.

[12] W. C. Chew and W. H. Weedon, *A 3D perfectly matched medium for modified Maxwell's equations with stretched coordinates*, Microwave Opt. Tech. Lett., 7 (1994), pp. 599–604.

[13] D. Colton and R. Kress, *Inverse Acoustic and Electromagnetic Scattering Theory*, 3rd ed., Springer, 2013.

[14] J. A. DeSanto and P. A. Martin, *On angular-spectrum representations for scattering by infinite rough surfaces*, Wave Motion, 24 (1996), pp. 421–433.

[15] M. Ehrhardt, H. Han, and C. Zheng, *Numerical simulation of waves in periodic structures*, Commun. Comput. Phys., 5 (2009), pp. 849–870.

[16] A. Fichtner, *Full Seismic Waveform Modelling and Inversion*, Springer, Berlin, 2011.

[17] S. F. Helfert and R. Pregla, *Efficient analysis of periodic structure*, J. Lightwave Technol., 16 (1998), pp. 1694–1702.

[18] G. Hu and A. Kirsch, *Time-harmonic scattering by periodic structures with Dirichlet and Neumann boundary conditions*, in preparation.

[19] G. Hu, W. Lu, and A. Rathsfeld, *Time-harmonic acoustic scattering from locally perturbed periodic curves*, SIAM J. Appl. Math., 81 (2021), pp. 2569–2595, https://doi.org/10.1137/19M1301679.

[20] Z. Hu and Y. Y. Lu, *Efficient numerical method for analyzing coupling structures of photonic crystal waveguides*, IEEE Photon. Tech. Lett., 21 (2009), pp. 1737–1739.

[21] S. Johnson, *Notes on Perfectly Matched Layers (PMLs)*, unpublished notes, https://math.mit.edu/~stevenj/18.369/spring09/pml.pdf, 2008.

[22] P. Joly, J.-R. Li, and S. Fliss, *Exact boundary conditions for periodic waveguides containing a local perturbation*, Commun. Comput. Phys., 1 (2006), pp. 945–973.

[23] T. Kato, *Perturbation Theory for Linear Operators*, reprint of the 1980 edition, Classics Math., Springer-Verlag, Berlin, 1995.

[24] A. Lechleiter and R. Zhang, *A Floquet-Bloch transform based numerical method for scattering from locally perturbed periodic surfaces*, SIAM J. Sci. Comput., 39 (2017), pp. B819–B839, https://doi.org/10.1137/16M1104111.

[25] W. Lu, *Mathematical analysis of wave radiation by a step-like surface*, SIAM J. Appl. Math., 81 (2021), pp. 666–693, https://doi.org/10.1137/20M1337338.

[26] W. Lu and Y. Y. Lu, *High order integral equation method for diffraction gratings*, J. Opt. Soc. Amer. A, 29 (2012), pp. 734–740.

[27] W. Lu and Y. Y. Lu, *Waveguide mode solver based on Neumann-to-Dirichlet operators and boundary integral equations*, J. Comput. Phys., 231 (2012), pp. 1360–1371.

[28] W. Lu and Y. Y. Lu, *Efficient high order waveguide mode solvers based on boundary integral*

equations, J. Comput. Phys., 272 (2014), pp. 507–525.

[29] W. Lu, Y. Y. Lu, and J. Qian, *Perfectly matched layer boundary integral equation method for wave scattering in a layered medium*, SIAM J. Appl. Math., 78 (2018), pp. 246–265, https://doi.org/10.1137/17M1112510.

[30] W. Lu, Y. Y. Lu, and D. Song, *A numerical mode matching method for wave scattering in a layered medium with a stratified inhomogeneity*, SIAM J. Sci. Comput., 41 (2019), pp. B274–B294, https://doi.org/10.1137/18M1182693.

[31] W. McLean, *Strongly Elliptic Systems and Boundary Integral Equations*, Cambridge University Press, Cambridge, UK, 2000.

[32] P. Monk, *Finite Element Methods for Maxwell's Equations*, Oxford University Press, New York, 2003.

[33] J. Sun and C. Zheng, *Numerical scattering analysis of TE plane waves by a metallic diffraction grating with local defects*, J. Opt. Soc. Amer. A, 26 (2009), pp. 156–162.

[34] L. Yuan and Y. Y. Lu, *A recursive doubling Dirichlet-to-Neumann map method for periodic waveguides*, J. Lightwave Technol., 25 (2007), pp. 3649–3656.

[35] W. Zhou and H. Wu, *An adaptive finite element method for the diffraction grating problem with PML and few-mode DtN truncations*, J. Sci. Comput., 76 (2018), pp. 1813–1838.